Excessive Cytokine and IgE Production in Murine *Hem1* Immunodeficiency Contributes to Allergic Airway Disease in a House Dust Mite Model

Julia Tsai

A thesis

submitted in partial fulfillment of the

requirements for the degree of

Master of Science

University of Washington

2025

Committee:

Brian M. Iritani

Jessica M. Snyder

Charles W. Frevert

Program Authorized to Offer Degree:

Comparative Medicine

University of Washington

Abstract

Excessive Cytokine and IgE Production in Murine *Hem1* Immunodeficiency Contributes to Allergic Airway Disease in a House Dust Mite Model

Julia Tsai

Chair of the Supervisory Committee:

Brian M. Iritani

Department of Comparative Medicine

Inborn errors of immunity (IEI) are a group of genetic diseases in humans that can present as increased susceptibility to infections, autoimmunity, hyperinflammation, allergic disease, and occasionally malignancy. A recently identified gene linked to IEI, *NCKAP1L,* encodes for Hematopoietic Protein-1 (HEM1), an adaptor protein which is critical for normal actin polymerization. Clinical investigation and immunophenotyping of HEM1 deficient children and murine models have documented similar characteristic features of IEIs, including recurrent infections and autoimmunity. However, the cellular mechanisms behind an increased prevalence of allergic airway disease (asthma) observed in HEM1 deficient children has not been further evaluated. In this study, we evaluated the development of asthma and primary immune cell populations and cytokines driving airway and lung pathology in various *Hem1* deficient mouse models. We hypothesized that Hem1 deficient T cells were driving asthma pathogenesis in part by increasing release of proinflammatory cytokines. Constitutive *Hem1* deficient mice (*Hem1*$^{-/-}$*),* conditional T cell specific *Hem1* deficient mice (*Hem1*$^{fl/fl}$*CD4Cre*), conditional B cell specific *Hem1* deficient mice (*Hem1*$^{fl/fl}$*Mb1Cre*), and age-matched control mice (10-25 week old males, n=5-8/group) received saline or house dust mite via the oropharyngeal route on days 0 and 14 for sensitization and days 26, 27, and 28 for challenge. On day 29, lungs, bronchoalveolar lavage fluid (BALF), and mediastinal lymph node were collected for flow cytometric analysis to identify representations of different myeloid and lymphoid cell populations.

Serum and supernatant of the BALF were analyzed for cytokine and IgE levels via multiplex immunoassay. Lungs were formalin-fixed for histopathologic evaluation using H&E and PAS staining. Our results indicate that in the face of allergic airway disease, *Hem1* deficient mice had decreased total numbers of myeloid and lymphoid immune cells in the airways, lung interstitium, and lymph node. However, Hem1 deficiency resulted in increased levels of asthma-related, proinflammatory cytokines (IL-17) and IgE in the BALF, resulting in asthma-related lung pathology. These results suggest that dysregulated cytokine and IgE production may contribute to asthma in Hem1 deficient humans and mice.

Table of Contents

Introduction

Inborn errors of immunity (IEI) are a group of diseases in humans that present with increased susceptibility to infections, autoimmunity, hyperinflammation, allergy, and possibly malignancy. A recently identified gene linked to IEI, *NCKAP1L* which encodes the protein Hematopoietic Protein-1 (HEM1), has been discovered as a hematopoietic cell specific component of the WASp family verprolin homologous (WAVE) actin regulatory complex (WRC). The WRC acts downstream of multiple immune receptors to stimulate F-actin polymerization, critical for cytoskeletal structures that drive most active cellular processes including migration, adhesion, immune synapse formation, and phagocytosis, all critical processes for an effective immune response.

In 2020, human patients from seven different lineages were identified with primary immune disorders (PID) secondary to loss-of-function (LOF) mutations in the *NCKAP1L* gene. These pediatric patients were shown to have improper actin polymerization secondary to loss of HEM1. Their clinical phenotype was overall variable although these children primarily suffered from recurrent bacterial and viral infections secondary to immunodeficiency and paradoxically, hyperinflammation, lymphoproliferation, atopy, and autoimmune disease.[1–4] Respiratory disease, in particular, was documented among these patients with recurrent upper respiratory tract infections, leading to bronchiectasis; cytokine hyperresponsiveness; and interstitial lung disease without a clear etiology. Five of the nine patients had atopic disease characterized by allergy, asthma, or eczema, highlighting an exaggerated atopic inflammatory response against environmental allergens and irritants with elevated IgE serum levels. Current clinical management of these patients includes immunomodulatory treatment, such as corticosteroids, cyclosporine, sirolimus, mycophenolate mofetil, and rituximab, and antibiotics for treatment of opportunistic infections.

Similar to their clinical variability, immunophenotyping of these HEM1 deficient patients also yielded variable differences in cell populations. Patients had decreased naïve T cells with increased central and effector memory cells and impaired CD4 T cell activation and proliferation, with variably increased CD8 T cell levels. On the other hand, B cells were normal to elevated in number, with an increase in a subset of B cells (termed “ABC” cells) associated with hyperinflammatory disease. In addition to elevations in IgE, elevated levels of IgG were noted in half of the patients. Finally, both T and B cells displayed abnormalities secondary to reduced actin polymerization with diminished cell spreading and lamellipodia formation at the immune synapse.[2–4]

Murine models of Hem1 deficiency have furthered understanding of human disease.[5] Investigation into the importance of Hem1 in the development and function of hematopoietic cells has found that loss of Hem1 not only drives immunodeficiency but also immune dysregulation. Similar to human patients, Hem1 deficient mice exhibited identical clinical features with increased failure to thrive, susceptibility to infectious agents, and diffuse hyperinflammation in various organs. These mice exhibited severe lymphopenia with impaired thymocyte development and reduced CD4, CD8, and γδ T cells in the periphery.[6] T cell activation and proliferation were also impaired; however, naïve T cells exhibited enhanced Th17 differentiation with an increased proportion of naïve T cells expressing IL-17 following culture in Th17 polarizing conditions (Christodoulou et al., in review). B cell specific deletion of *Hem1* in *Hem1*$^{fl/fl}$*Mb1Cre*$^{+}$ mice showed that *Hem1* is important for development of murine B cells and generation of protective antibody responses against T cell independent antigens.[7] B cells were also found to be significantly reduced in the bone marrow and periphery. Conversely, B cells were found to be more activated both basally and following B cell receptor stimulation, and T cell dependent antibody responses from B cells were more robust with increased production of IgM and IgG after antigen exposure. Autoantibody production was also increased, which correlated with increased proportions of "ABC" like cells, as was noted in Hem1 deficient humans.

In the myeloid cell population, Hem1 deficient neutrophils, monocytes, and macrophages were found to have impaired phagocytosis and migration.[8] More specifically, constitutive *Hem1*$^{-/-}$ mice and myeloid cell specific *Hem1* deficient *Hem1*$^{fl/fl}$*LysMCre* mice developed accumulation of excessive mucus and cell debris in the airways, leading to alveolar proteinosis, and alveolar macrophages in the lungs exhibited a shift towards a proinflammatory, immature phenotype.[9] Hem1 deficient dendritic cells (DCs) acquired an abnormal needle-like morphology compared to wild-type DCs, affecting their ability to migrate to lymph nodes from peripheral tissues due to defective interstitial crawling and intravasation. Loss of Hem1 in dendritic cells also affected cell-to-cell interactions with other leukocytes, such as T cells, due to decreased actin content at the immunological synapse. Affected dendritic cells demonstrated increased contact time with T cells, resulting in fewer overall T cell:DC interactions and fewer activated T cells. However, once activated, T cells did not show differences in proliferation or IL-2 production compared to those activated by wild-type DCs.[10,11]

Allergic disease and atopy in HEM1 deficient patients have not been further evaluated, and bronchodilators are the main mode of asthma management in these children. Asthma, however, is a heterogeneous lung disease with variable clinical presentations (phenotypes) and distinctive endotypes (mechanisms), attracting considerable effort to understand the mechanisms driving the disease. Key characteristics of asthma include variable airflow

obstruction and airway hyperresponsiveness (AHR), causing episodic and reversible bronchoconstriction. However, the exact pathologic mechanisms are complex and associated with variable factors such as different environmental triggers, age, obesity, and genetic factors. The majority of research has focused on understanding the aberrant $CD4^+$ T helper type 2 (Th2) inflammation mediated by associated Th2 cytokines (IL-4, IL-5, and IL-13). However, recently, the disease has been classified into Th2-high and Th2-low asthma, acknowledging that airway disease can be driven by mixed inflammation.[12] Th2-high asthma is characterized by eosinophilic airway inflammation with increased blood eosinophil counts or elevations in fractional exhaled nitric oxide (FeNO). Th2-low asthma instead includes neutrophilic or paucigranulocytic asthma with IL-17, TNFα, and IFNγ proposed as major cytokines in the pathogenesis. Through this distinct classification, key disease biomarkers, such as IgE levels, FeNO levels, cytokine levels, blood total eosinophil count, or sputum neutrophils, are used for diagnosis, classification and treatment guidance.

In this study, we investigated the pathogenesis behind the increased incidence of asthma in HEM1 IEI patients, by modeling the disease in *Hem1* deficient mice using house dust mite antigen (HDM) delivered via the oropharyngeal route. Our results show that despite decreased representation of most immune cells in bronchoalveolar lavage fluid (BALF) and lung tissue in *Hem1* deficient vs control mice following HDM exposure, BALF from *Hem1* deficient mice contained increased levels of IL-13, IL-17, and IgE. This correlated with increased IL-13, IL-17, and TNFα production following in vitro TCR stimulation of purified splenic $CD4^+$ T cells from $Hem1^{fl/fl}CD4Cre^+$ vs control mice. These results suggest that LOF variants in NCKAP1L may predispose to asthma and perhaps other atopic diseases in part by skewing T helper cell differentiation towards Th2 and Th17 production, characteristics of both Th2 high and Th2 low asthma.

Material and Methods

Animals

All experiments were approved by the University of Washington Institutional Animal Care and Use Committee (IACUC). Mice were bred in house. Due to the potential for phenotypic differences between males and females in the development of asthma, male mice between the ages of 16-26 weeks were used in all experiments. Littermate controls were utilized whenever possible and in most experiments.

Constitutive *Hem1*$^{-/-}$, *Hem1*$^{fl/fl}$*Mb1Cre* (i.e., B cell specific deletion of *Hem1*), and *Hem1*$^{fl/fl}$*CD4Cre* (i.e., immune cell – T cell and monocyte deletion of *Hem1*) mice were generated as previously described.[6,7,9] Animals were housed on a 14:10 light:dark cycle within the University of Washington animal care facilities. Animals were given free access to food (Irradiated PicoLab Rodent Diet 5053; LabDiet, St. Louis, MO) and water (reverse osmosis purified, chlorinated). Animals were housed in autoclaved individually ventilated cages (Allentown Inc., Allentown, NJ) with autoclaved corn cob bedding (The Andersons, Maumee, OH) and free access to nesting materials (Nestlets; Ancare, Bellmore, NY). Mice were maintained specific-pathogen free via a rodent health-monitoring program that excludes: Pinworms; Fur mites; Mouse coronavirus (MHV); Mouse parvovirus (MPV); Minute virus of mice (MVM); Murine rotavirus (MRV/EDIM); Reovirus-3 (Reo-3); Sendai virus; Pneumonia virus of mice (PVM); Theiler's murine encephalitis virus (TMEV); Ectromelia (mousepox); Lymphocytic choriomeningitis virus (LCMV); Mouse adenovirus type 1 and type 2 (MAV 1 and 2); Murine cytomegalovirus (MCMV); *Mycoplasma pulmonis*; and *Corynebacterium bovis*.

Asthma Induction via House Dust Mite (HDM) Regimen

House dust mite (*Dermatophagoides pteronyssinus*) extract (Stallergenes Greer, Lenoir, NC) was dissolved in sterile saline (Aspen Veterinary Resources, Loveland, CO). Mice were anesthetized via isoflurane (Patterson Veterinary Supply, Houston, TX) and administered either saline or HDM extract in saline oropharyngeally. To induce allergic airway disease, HDM was administered on day 0, day 14, day 26, day 27, and day 28 as previously described.[13] On days 0 and 14, mice received 100μg of HDM protein via 50μl of saline while on days 26, 27, and 28, mice received 50μg of HDM protein via 50μl of saline (Figure 1). For the control treatment, mice were administered 50μl saline following the same timeline. Mice were euthanized on day 29.

Complete Blood Count (CBC) Analysis

Blood was collected from wild-type and *Hem1KO* mice via the submandibular vein in BD Microtainer K2EDTA tubes, and complete blood count analysis was performed on 200ul of whole blood by IDEXX Laboratories, Inc. (Westbrook, Maine).

In Vivo Antibody Labeling and Tissue Harvest

For the *Hem1KO* mice, antibody staining and tissue harvest of the lungs, bronchoalveolar lavage fluid (BALF), and mediastinal lymph node (MLN) followed the steps, previously described in detail.[13]

For the *Hem1CD4Cre* and *Hem1Mb1Cre* cohorts, mice were euthanized via carbon dioxide asphyxiation. The trachea was cannulated with an 18-gauge angiocath via tracheostomy, and airways were lavaged with 1ml of cold PBS three times. The supernatant from the first lavage was stored at − 80 °C until use. The cells from all three lavages were pooled and analyzed via flow cytometry. The thoracic cavity was opened via midline sternotomy. Under a dissecting microscope, the largest mediastinal lymph node was removed from the dorsal aspect of the trachea. The lymph node was placed directly in PBS containing 2% fetal bovine serum (FBS, Thermo Fisher Scientific Waltham, MA) on ice.

Flow Cytometry

For the *Hem1KO* mice, preparation of single-cell suspensions of the lungs, BALF, and MLN and flow cytometric analysis followed the steps as described in detail previously.[13]

For the *Hem1$^{fl/fl}$CD4Cre* and *Hem1$^{fl/fl}$Mb1Cre* cohorts, cells collected via bronchoalveolar lavage were pelleted and resuspended in PBS containing 2% FBS. Mediastinal lymph nodes were transferred to 70 μm cell strainers and gently mashed with the rubber end of the plunger from a 3-ml syringe. The filters were rinsed with 5ml of PBS containing 2% FBS. Cells were counted manually via hemocytometer using Trypan Blue. Cells were stained with fluorescent dye-conjugated antibodies, including the following: CD45.2 (PCP Cy5.5), Ly6G (APC Cy7), CD11c (PE), CD11b (PB), F4/80 (APC), SiglecF (FITC), Ly6c (PE Cy7), CD45.2 (FITC), CD4 (APC), CD8 (PE Cy7), CD3 (PerCP Cy5.5), CD19 (PE). See gating strategy in Supplemental Figure 1.

IgE and Cytokine Assays

Bronchoalveolar lavage supernatant was collected and analyzed for IgE, cytokine, and chemokine levels using the Mouse Immunoglobulin IgE Single Plex Assay (MGAM-E-108) and Mouse Cytokine/Chemokine 32-Plex Discovery Assay® Array (MD32) (Eve Technologies, Calgary, AB), respectively.

T cell stimulation

Splenocytes from *Hem1*$^{fl/fl}$*CD4Cre*$^{+}$ and control mice were enriched for T cells by positive selection of CD4^{+} T cells (CD4 (L3T4) MicroBeads, Miltenyi Biotec), and equal numbers of cells were stimulated with 15μg/ml of anti-CD3 (17A2, Biolegend) and anti-CD28 (37.51, Biolegend) antibody-coated plates for 72 hours in complete RMPI media (RPMI + L-glutamine, 10% FBS, 1% penicillin streptomycin, 1% MEM amino acids, 1% sodium pyruvate, 0.1% 2-mercaptoethanol). Supernatant was collected and analyzed for cytokine and chemokine levels using the Mouse Cytokine/Chemokine 32-Plex Discovery Assay® Array (MD32) (Eve Technologies, Calgary, AB).

Histopathology Analysis

Lungs were inflated with 1ml of 10% buffered neutral formalin and then placed in 10% buffered neutral formalin. After routine paraffin embedding, 4μm sections were stained with hematoxylin and eosin (H&E) to evaluate inflammatory changes around the airways and blood vessels and within the interstitium and alveolar spaces. To examine changes in mucus production and goblet cell hyperplasia, sections were stained with Periodic Acid Schiff (PAS). All histopathological analyses were conducted by a board-certified veterinary pathologist, blinded to genotype and treatment. Lung lesions were graded following a modified system from a previously described protocol.[14] In addition to the evaluation of perivascular and peribronchial inflammation, H&E slides were evaluated for alveolar and interstitial inflammation. Interstitial inflammation was evaluated using a semi-quantitative scale of 0-4, with 0 representing no relevant inflammatory changes and 4 representing severe, multifocal to coalescing to diffuse interstitial pneumonia. Similarly, alveolar inflammation was evaluated from 0-4, with 0 representing no relevant inflammatory changes and 4 representing greater than 50% of the alveoli are filled with degenerative neutrophils and histiocytes including multi-nucleated giant cells and fibrin. PAS-stained sections were scored from 0-4, reflecting <5%, 5-25%, 26-50%, 51-75%, and >76% mucus positive epithelial cells per bronchiole, respectively.

Histology images were captured from glass slides using NIS-Elements BR 4.20.01 and images of gross and histologic lesions were plated in Adobe Photoshop 2023. Image white balance, contrast and lighting were adjusted using auto-corrections applied to the entire image.

Immunohistochemistry

Immunohistochemical (IHC) staining was performed using an indirect immunoperoxidase technique with diaminobenzidine (DAB) as the chromogen for cleaved-caspase 3 (CC3) (Cell Signaling Technology, Danvers, MA, Rabbit mAb #9579, dilution 1:250). IHC staining was performed using an autostainer (Leica Bond Automated

Immunostainer, Leica Biosystems, Deer Park, IL). Processed slides were deparaffinized on the Leica Bond Automated Immunostainer. Endogenous peroxidase activity was blocked with Leica Bond Peroxide block at room temperature for 5 minutes, incubated for 20 minutes at room temperature with TBS with 10% normal goat serum. Slides were incubated with CC3 for 30 minutes at room temperature. The detection system used was the Leica BOND Polymer Refine detect, and the reaction was developed using DAB. Slides were counterstained with hematoxylin.

Image analysis was performed following immunohistochemistry using whole-slide digital images and automated image analysis. Brightfield whole slide digital images were created using a 20x objective and the Nanozoomer Digital Pathology slide scanner (Hamamatsu, Bridgewater, NJ). Analysis of the whole-slide digital images was performed using Visiopharm software (Visiopharm, Hoersholm, Denmark). Regions of interest (ROIs) were manually defined by drawing around the visible area of lung tissue. Digital features were trained to label positive staining for CC3 markers and the background tissue counterstain (hematoxylin) using project-specific configurations based on a threshold of pixel values. Images were processed to generate desired outputs (area of positive staining for CC3 as a ratio of positive staining to total tissue area). All ROIs were sampled at 100%.

Statistics

Data were analyzed using the Student's 2-tailed unpaired t test with equal variance, using GraphPad Prism 9. Normality was assessed using the Shapiro-Wilk normality test, and nonparametric data were analyzed using the Mann-Whitney u test using GraphPad Prism 9. $P < 0.05$ was considered significant. All graphs show mean with standard error of the mean (SEM).

Results

Compartmental Analysis of the Pulmonary Immune Response in *Hem1* deficient mice with house dust mite induced asthma

To model asthma in *Hem1* deficient mice, we delivered HDM or saline to 16-26 week old *Hem1*$^{-/-}$ (*Hem1KO)* and *Hem1*$^{+/-}$ control mice on days 0, 14, 26, 27, and 28. Before euthanasia, mice were anesthetized with isoflurane, and CD45.2 was injected retro-orbitally to label intravascular (IV) leukocytes (IVCD45^{+}). After 3 minutes, the left renal artery was transected, and the trachea was cannulated with an 18-gauge angiocath via tracheostomy and CD45.2 (different fluorophore) was instilled via intratracheal instillation into the lungs (ITCD45^{+}) and allowed to remain for 3 minutes. The airway was lavaged two additional times, and the lungs were then perfused via injection of PBS into the right ventricle. Mediastinal lymph node and lung tissue were then collected for spectral flow cytometric analyses.[13]

All cell populations were characterized as previously described (Figure 1A, right) and reiterated in brief here: neutrophils Ly6G^{+}; lymphoid Ly6G^{+} CD64^{-} F4/80^{-}, non-lymphoid CD64^{+} or F4/80^{+}. Within the lymphoid population, the T cell population is characterized as CD3e^{+}, CD4^{+} T helper; CD3e^{+}, CD8^{+} Cytotoxic T; CD3e^{+}, CD4^{-} CD8^{-} γδTCR^{+} γδ T cells. Other lymphoid cells include CD19^{+} MHCII^{+} B cells and CD3e^{-} CD19^{-} CD49b^{+} NKp46^{+} NK cells. Within the non-lymphoid population, macrophages are characterized as CD64^{hi} F4/80^{hi} and include CD11b$^{lo/mid}$ CD11c^{hi} SiglecF^{+} Alveolar Macrophages, CD11b^{hi} CD11c$^{lo/mid}$ MHCII^{+} SiglecF^{-} Recruited Macrophages, and CD11b^{hi} CD11c$^{lo/mid}$ MHCII^{-} SiglecF^{-} Mono-Macrophages. Non-macrophages CD64$^{lo/int}$ F4/80$^{lo/int}$ include CD11c^{+} MHCII^{+} Dendritic cells, C11c^{-} MHCII^{-} SiglecF^{-} SSC^{lo} CD11b^{+} Ly6C$^{lo\&hi}$ Monocytes, and C11c^{-} MHCII^{-} SiglecF^{+} SSC^{hi} Eosinophils.[13]

Hem1KO mice had significantly fewer cells in the bronchoalveolar lavage fluid secondary to reduced myeloid cell populations (Figure 1B and Supplemental Figure 2A). Of this myeloid population, *Hem1KO* mice had significantly decreased eosinophils, macrophages, mono-macrophages, and dendritic cells (Figure 1B). Both wild-type and KO mice showed similar levels of lymphoid cells with similar B cell populations; however, there was a significant decrease in NK cells in *Hem1KO* mice.

Of the non-lavageable airway, termed the adherent airway, *Hem1KO* mice had significantly reduced cell populations, mainly characterized by decreased myeloid cells. Similar to the bronchoalveolar lavage cells, *Hem1KO* mice showed significantly fewer eosinophils and mono-macrophages (Figure 2 and Supplemental Figure 2B). Dendritic cells and macrophages also showed a decrease in cell number, but this difference was not

statistically significant (p = 0.09 and 0.21, respectively). Both wild-type and KO mice showed similar numbers of B and T cells; however, NK cells were significantly decreased in the *Hem1KO* mice.

Within the marginated lung vasculature (as labeled by intravascular CD45.2), the lymphoid cell population of *Hem1KO* mice was significantly reduced while the myeloid population was similar to wild-type mice. Within the lymphoid populations, *Hem1KO* mice showed significantly decreased B cells, $CD4^+$ and $CD8^+$ T cells, $\gamma\delta$ T cells as well as NK cells (Figure 3 and Supplemental Figure 2C). There were no significant differences in myeloid cell populations, including eosinophils and dendritic cells.

Within the lung interstitium, myeloid and lymphoid cell populations were not significantly different; however, *Hem1KO* mice had significantly decreased eosinophils, NK cells, and B cells (Figure 4 and Supplemental Figure 3A).

Evaluation of the cell populations within the mediastinal lymph node showed significantly reduced populations of lymphoid and myeloid cells. Within the myeloid cell populations, *Hem1KO* mice had fewer eosinophils, macrophages, mono-macrophages, and monocytes while the lymphoid population showed a significant decrease in B cells, $CD4^+$ and $CD8^+$ T cells, $\gamma\delta$ T cells, as well as NK cells (Figure 5 and Supplemental Figure 3B).

Overall, the changes in the *Hem1KO* mice compared to controls showed a reduction in myeloid cells, specifically eosinophils in various tissue compartments (airways and lung interstitium). Additionally, lymphoid populations ($CD4^+$ T and B cells) were significantly decreased in the lung vasculature and mediastinal lymph node. These cell populations, key to the immune response in the development of asthma, suggested initially that *Hem1KO* mice could have a less severe asthmatic phenotype.

Baseline bloodwork and Compartmental Analysis of the Pulmonary Immune Population in *Hem1* deficient mice with saline administration

To determine if any of the alterations in cell populations occurred independent of HDM treatment, we administered saline following the regimen shown in Figure 1A and performed similar spectral flow analysis. We also evaluated the baseline systemic leukocyte population of our *Hem1KO* mice via CBC to determine if a systemic reduction of leukocytes could explain the reduced populations in airways.

Complete blood count of *Hem1KO* and wild-type mice at baseline with no administration of substances was performed to evaluate the systemic circulating white blood cell (WBC) population (Figure 6). *Hem1KO* mice have significantly decreased percentages and total numbers of eosinophils and lymphocytes per μl of blood. In contrast, the percentage of

neutrophils in the WBC population was increased although the overall neutrophil cell count per μl was not significantly different between *Hem1KO* and wild-type mice.

In the bronchoalveolar lavage fluid and the mediastinal lymph node, *Hem1KO* and wild-type mice had similar numbers of the cell populations evaluated (Supplemental Figures 4 and 5, respectively). Of the non-lavageable airway, *Hem1KO* mice had significantly decreased alveolar macrophages and eosinophils (Supplemental Figure 6).

Within the marginated lung vasculature, the lymphoid and myeloid cell populations of *Hem1KO* mice were significantly reduced (Supplemental Figure 7). Within the myeloid population, neutrophils, eosinophils, and cells of the macrophage lineage (macrophages, alveolar macrophages, recruited macrophages, mono-macrophages) were significantly decreased. Of the lymphoid population, *Hem1KO* mice showed significantly fewer $CD4^+$ and $CD8^+$ T cells, γδ T cells, B cells, as well as NK cells. Dendritic cells also showed a reduction in cell number, but this difference was not statistically significant ($p = 0.05$).

Within the lung interstitium, myeloid and lymphoid cell populations were not significantly different; however, *Hem1KO* mice had significantly increased monocytes but similar numbers of macrophage populations (Supplemental Figure 8).

Lung Histopathology in *Hem1* deficient mice with house dust mite induced asthma

We next evaluated lung pathology via histology in *Hem1* deficient mice following exposure to HDM. Despite a reduction of most immune cell populations via flow cytometry, we found that *Hem1KO* mice showed significantly increased lung pathology. *Hem1KO* mice showed significantly increased alveolar and interstitial inflammation compared to wild-type mice while histologic scores for perivascular and peribronchial inflammation were similar (Figure 7A). Additionally, IHC analysis for apoptosis showed that lungs of *Hem1KO* mice had a significantly increased percent of cleaved caspase-3 (CC3) positive cells (Figure 8).

To rule out underlying pulmonary infection as the cause of increased inflammation in our *Hem1KO* mice, HDM administration was performed in wild-type and *Hem1KO* mice concurrent with systemic oral antibiotics (enrofloxacin via the drinking water), and subsequent lung histopathology was evaluated (Figure 7B). In the *Hem1KO* mice that received antibiotic administration during HDM sensitization, there were similar findings of increased histologic severity of alveolar inflammation but equal severity of interstitial, perivascular, and peribronchial inflammation as compared to the wild-type mice.

PAS staining of bronchiole epithelial cells showed similar numbers of mucus secreting cells between *Hem1KO* mice and wild-type mice with or without concurrent antibiotic

administration. Representative PAS staining is shown for the cohort of mice that did not receive concurrent antibiotics (Supplemental Figure 9).

Cytokine and IgE Analysis of Bronchoalveolar lavage fluid of mice at baseline and with house dust mite induced asthma

Given the increase in histologic pulmonary inflammation seen in *Hem1* deficient mice following HDM exposure, we next evaluated whether alterations in cytokine production may be a contributing factor. We assessed cytokine production in BALF from *Hem1KO* and control mice following either saline or HDM exposure via a multiplex bead cytokine array, which assesses 32 cytokines (Eve technologies).

In the BALF of *Hem1KO* mice with saline administration, of the Th2 high cytokines, IL-13 and eotaxin concentrations were significantly increased at baseline with saline administration (Figure 9A). IL-17 was also significantly increased compared to wild-type mice (Figure 9B). IL-6 also showed elevated levels in the *Hem1KO* mice, but this difference was not statistically significant ($p = 0.06$).

In the BALF of *Hem1KO* mice with HDM induced asthma, wild-type and *Hem1KO* mice showed similar concentrations of IL-4, IL-5, IL-13, eotaxin, and IL-9, indicating that Th2 high cytokines had similar robust Th2 responses in the face of HDM (Figure 9C). However, the BALF of the *Hem1KO* mice had significantly elevated IgE levels compared to wild-type mice with HDM administration. IL-17, a Th2 low cytokine, was significantly elevated compared to wild-type mice, as was seen in saline treated mice. TNFα, another Th2 low cytokine, was also significantly elevated (Figure 9D). These results suggest that despite a reduction of most immune cells, disruption of Hem1 resulted in increased levels of important asthma inducing proinflammatory cytokines, including both Th2 high and Th2 low cytokines in the absence of HDM, which were further exacerbated by HDM administration.

Hem1 deficiency predisposes to CD4 T cells to skew towards Th17 and Th2 phenotypes.

The increase in IL-17 and IL-13 in *Hem1* deficient mice in the absence of HDM, suggested that perhaps loss of *Hem1* may predispose T cells towards Th17 or Th2 cell fates. To examine this hypothesis, we purified total $CD4^+$ T cells from *Hem1*$^{fl/fl}$*CD4Cre*$^+$ and control mice and assessed cytokine production following anti-CD3/CD28 stimulation for 72 hrs. Cytokines associated with TH2 T cells, IL-13 and IL-9, were significantly elevated in the supernatant of stimulated *Hem1* deficient $CD4^+$ T cells compared to control $CD4^+$ T cells (Figure 10A). Additionally, IL-17 was significantly elevated, and TNFα, a cytokine associated with Th2 low asthma and Th1 inflammation, also showed an increased concentration though this difference was not statistically significant ($p = 0.096$). Additional cytokines and

chemokines that have been previously implicated in asthmatic patients or murine models of asthma were significantly increased, including Rantes, MIP-1β, MIP-2, and MCP-1, chemokines for various myeloid cell populations including eosinophils, neutrophils, and monocytes/macrophages (Figure 10B).[15] These results indicate a pro-inflammatory role of the *Hem1* deficient $CD4^+$ T cells upon stimulation that could lead to more severe lung pathology. Interestingly, we also found elevations in IL-10 and IL-12p70 in *Hem1* deficient $CD4^+$ T cells, indicating a strong T-regulatory and Th1 response, respectively that could either dampen the overall inflammatory response or the Th2 specific immune response in *Hem1* deficient mice. Finally, asthmatic patients have been shown to have increased levels of VEGF, which has been shown to induce Th2 inflammation and parenchymal and vascular remodeling. The significant decrease in production from *Hem1* deficient $CD4^+$ T cells may act as a protective effect during the development and pathogenesis of asthma.[16,17]

Neither T cell nor B cell specific disruption of Hem1 alone predispose to allergic airway disease.

Because of the dramatic increase in T cell derived cytokines and increased B cell derived IgE, we next sought to evaluate if loss of *Hem1* only in T cells or B cells might be impactful enough to drive the development of asthma. To test this, we administered saline and HDM to $Hem1^{fl/fl}CD4Cre^+$ and $Hem1^{fl/fl}Mb1Cre^+$ mice following the same regimen. Similar to our initial experiment with our *Hem1KO* mice, we evaluated the immune cell population of the mediastinal lymph node and bronchoalveolar lavage fluid, cytokine levels in the BALF, and lung histopathology. In this experiment, two smaller flow panels were utilized to identify the lymphoid and myeloid populations in each tissue (Supplemental Figure 1). The lymphoid population was characterized by: $CD45.2^+$ $CD4^+$ T cells, $CD45.2^+$ $CD8^+$ T cells, $CD45.2^+$ $CD8^-$ $CD4^-$ $CD19^+$ B cells while the myeloid population consisted of: $CD45.2^+$ $Ly6G^+$ Neutrophils, $CD45.2^+$ $Ly6G^-$ $F4/80^{lohi}$ $CD11c^-$ $SiglecF^+$ Eosinophils, $CD45.2^+$ $Ly6G^-$ $F4/80^{lohi}$ $CD11c^+$ $SiglecF^+$ Alveolar macrophages, and $CD45.2^+$ $Ly6G^-$ $F4/80^{lohi}$ $CD11c^-$ $SiglecF^-$ SSC^{lo} $CD11b^+$ Monocytes.

With saline administration, the BALF of $Hem1^{fl/fl}CD4Cre^+$ mice did not show significant differences in cell population compared to control mice ($Hem1^{fl/fl}CD4Cre^-$); however, in the mediastinal lymph node, there was a significant reduction in $CD4^+$ and $CD8^+$ T cells (Supplemental Figure 10). After HDM administration, $Hem1^{fl/fl}CD4Cre^+$ mice showed significantly decreased numbers of $CD8^+$ T cells in the BALF and increased B cells in the MLN (Supplemental Figure 11). There were no significant differences in cytokine production in either the saline or HDM cohorts (Supplemental Figure 12). Similarly, $Hem1^{fl/fl}CD4Cre^+$ mice do not appear to have significant differences in baseline lung pathology or inflammation compared to control mice, and with HDM administration, exhibit significantly

decreased peribronchial inflammation compared to control mice (Supplemental Figure 13).

For *Hem1*$^{fl/fl}$*Mb1Cre*$^{+}$ mice that received HDM, the B cell population was significantly decreased in the BALF and the MLN with no other significant changes in cell population (Supplemental Figure 14). Cytokine levels in the BALF also did not show significant differences (Supplemental Figure 15). While there were no significant histologic differences in inflammation between the *Hem1*$^{fl/fl}$*Mb1Cre*$^{+}$ and control mice (data not shown), on evaluation, control mice had more robust lymphocytic cuffs with admixed polymorphonuclear cells, likely neutrophils and eosinophils while the *Hem1*$^{fl/fl}$*Mb1Cre*$^{+}$ mice had more alveolar and interstitial disease, similar to our *Hem1KO* cohort.

Discussion

In this study, we investigated the predisposition of children with loss of HEM1 to develop atopic disease or allergic disease, specifically asthma. Utilizing a mouse model of HDM-induced asthma in our constitutive *Hem1KO* mice, we evaluated the main cell populations and cytokines that may be driving lung pathology and allergic airway disease. In the face of allergic airway disease, *Hem1KO* mice showed elevated cytokine levels (IL-17, TNFα) and IgE in their BALF despite a decrease in eosinophils in the airways and a decreased lymphoid population in the lung vasculature and mediastinal lymph node. Interestingly, this imbalance of cytokines likely contributed to increased or similar levels of pulmonary inflammation and apoptosis in our *Hem1* deficient mice. Given the potential role of $CD4^+$ T helper cells in driving the asthmatic immune response, in vitro stimulation of *Hem1* deficient $CD4^+$ T cells was performed and showed elevations in both pro-inflammatory (Th2 and Th17) cytokines and chemokines and anti-inflammatory cytokines that are likely contributing to the inflammatory milieu of the pulmonary system during exposure to HDM antigen. These findings lead us to conclude that a combination of Th2 and Th17 immune responses are driving the development and severity of asthma in *Hem1* deficiency.

Allergic asthma is characterized as a chronic inflammatory disease with reversible airway obstruction, airway hyperresponsiveness, eosinophilia, a $CD4^+$ Th2 or Th17 lymphocyte dominated immune response, and elevated serum IgE levels.[18] Upon allergen exposure, airway epithelial cells produce chemokines and cytokines (IL-1, GM-CSF, IL-33) to activate type 2 innate lymphoid cells and dendritic cells.[19] Once dendritic cells migrate to the mediastinal lymph node for antigen presentation, they induce Th2 cell differentiation, and Th2 derived cytokines, mainly IL-4, will activate B cells and promote immunoglobulin class switching to IgE. Circulating IgE can then bind to high affinity IgE receptors (FcεRI), crosslinking complexes on mast cells (tissue-resident) and basophils (found in the peripheral blood). Mast cell and basophil degranulation will immediately release inflammatory mediators, such as histamine and other cytokines that can recruit granulocytes, such as neutrophils and eosinophils, induce smooth muscle contraction and mucus secretion, and trigger cytokine production from endothelial cells.[20–22]

As previously published, in the naïve or PBS administered lung, the primary cells of the marginated vasculature include neutrophils, monocytes, and eosinophils of the myeloid population and a smaller proportion of B, T helper, and NK cells of the lymphoid population.[13,23] The overall decrease in myeloid (macrophages, eosinophils, and neutrophils) and lymphoid cells (T cells, B cells, and NK cells) present in the marginating lung vasculature of the saline administered *Hem1KO* mice also suggests that the naïve *Hem1KO* lung may not have a large pool of immune cells ready to rapidly enter the

interstitium in response to infection or injury. This may be due to defective migration of Hem1 deficient myeloid cells and lymphocytes from peripheral blood into peripheral tissues, which has previously been noted. Of note, however, the *Hem1KO* mice actually have similar numbers of monocytes in the marginating lung vasculature and significantly increased numbers in the lung interstitium, indicating the presence of a key phagocytic effector and precursor cell likely participating in steady-state surveillance of the lung airways and vasculature.[24]

The most striking difference in our *Hem1KO* mice compared to control mice when administered saline or HDM was the lack of eosinophils in various tissue compartments. In the systemic circulation at baseline, *Hem1KO* mice had decreased eosinophil and lymphocyte counts with a resulting increased proportion of neutrophils. Despite this increased proportion of neutrophils in the systemic circulation, we did not see an increased neutrophil population in the lungs with saline or HDM administration, suggesting impaired migration, survival, and/or adhesion. Additionally, for eosinophils, the decreased number was also reflected in the adherent airway and marginating lung vasculature but not the BALF in our investigation of the baseline lung immune cell population. This decrease in eosinophils from the adherent airways but not the BALF could represent a de facto decrease in adherent eosinophils in our *Hem1KO* mice or a shift of eosinophils from the non-lavageable to the lavageable airway due to disrupted integrin-mediated adhesion as has been shown in *Hem1* deficient macrophages.[25] The decrease in eosinophils in the systemic circulation and lung vasculature could suggest decreased production from the bone marrow, decreased survival in circulation, or increased sequestration in various organs, such as the lung, spleen, or gastrointestinal tract. However, similar eosinophil counts within the lung interstitium between our *Hem1KO* and control mice suggests an unaffected tissue-resident population within the lungs. This tissue-resident eosinophil population has been shown to play a regulatory role for homeostasis within the lung and does not contribute to HDM-induced airway allergy. Mice lacking these regulatory eosinophils will develop an increase in Th2 cell response to inhaled allergens, as tissue-resident eosinophils can inhibit the maturation of allergen-presenting dendritic cells.[26]

With the HDM model of murine asthma, a Th2-polarized response is critical for lung cytokine production, airway hyperresponsiveness, and airway remodeling.[27] In particular, this model drives an influx of eosinophils and Th2 cells to the lungs and the airway lumen.[15] However, in *Hem1KO* mice, there appears to be a lack of migration of eosinophils into the lung interstitium and the airways. Compared to control mice, *Hem1KO* mice in the face of HDM-induced asthma have a significantly decreased eosinophil population in the airways and lung interstitium. However, the levels in the marginated lung vasculature are similar to those of control mice, suggesting that eosinophils from the systemic circulation are

responding to inflammatory signaling from the pulmonary endothelium, which attracts and activates circulating eosinophils in asthma.[17] Interestingly, this inflammatory eosinophil subpopulation that is distinct from the tissue-resident regulatory population is not able to migrate from the lung vasculature to the airways and interstitium as seen on flow cytometry.[26]

Another key subset of immune cells in the Th2 immune response are adaptive lymphoid cells, mainly $CD4^+$ T cells and B cells. The transition from the innate to adaptive immune response in asthma is facilitated by antigen presenting cells (APCs), mainly alveolar macrophages and dendritic cells. While alveolar macrophages play a role in the uptake of airway HDM, the transport of HDM to the mediastinal lymph node requires active cellular transport via dendritic cells.[28] This recruitment and migration of specifically dendritic cells to the draining lymph node to interact with naïve T cells is fundamental in instructing both humoral and Th2 mediated immune responses.[29] Once differentiated, allergen-specific Th2 cells traffic to the lungs, where they rapidly release cytokines, feeding the inflammatory feedback loop.[30] In addition to IgE production, B cells also perpetuate the adaptive immune response by exhibiting an accessory role in antigen presentation and T cell activation in the lymph node.[18,29]

With administration of HDM in our *Hem1KO* mice, lymphoid cells are still significantly decreased in the marginating lung vasculature; however, the myeloid population of the *Hem1KO*, likely responding to inflammatory chemokines, is similar to that of the control mice. In the lung parenchyma, B cells are significantly decreased, and in the mediastinal lymph node, dendritic cells, $CD4^+$ T cells, and B cells are significantly decreased. Similar to our mice, previous work has shown a reduced proportion of $CD4^+$ T cells in the peripheral lymph nodes of a murine model of *Hem1* deficiency, suggesting poor migration of immune cells to the LN, (Christodoulou et al., unpublished) and reduced effector function in HEM1 deficient $CD4^+$ T cells in human patients.[2,3] Additionally, these *Hem1* deficient T cells had impaired T cell immune synapse formation, potentially leading to decreased signaling following T cell receptor binding and reduced activation and effector function (Christodoulou et al., in review). In evaluation of *Hem1* deficient dendritic cells, similar impairment of the actin cytoskeleton led to decreased activation of T cells due to imbalanced DC-T cell contact, and affected dendritic cells also had impaired chemokine driven migration through complex tissue environments.[10,11] In combination, the poor migratory and effector ability of *Hem1* deficient dendritic cells to activate $CD4^+$ T cells in the mediastinal lymph node likely contributed to the decreased dendritic cell, B cell, and T cell populations seen with asthma and potentially could suggest a poor adaptive immune response to HDM allergy.

However, despite this distinct decrease in immune cells related to a Th2 high response (eosinophils in the lungs and airways, dendritic cells and adaptive immune cells in the lymph node), the *Hem1KO* mice still exhibited a similar severity of pulmonary inflammation (peribronchial and perivascular) as the control mice. While IHC staining of CC3 demonstrated increased apoptosis of this inflammatory cell population, which could explain the discrepancy between our flow cytometric and histologic results, we believe this inflammatory cell population is still driving lung pathology via cytokine and IgE expression. Repeated exposure of HDM produces progressive airway inflammation in BALB/c mice with peribronchialar and perivascular infiltrates of eosinophils, neutrophils, and lymphocytes. After 7 days of repeated intranasal HDM administration, thick perivascular cuff and bronchialar epithelial hypertrophy and hyperplasia are observed with eventual development of perivascular edema and goblet cell hypertrophy and hyperplasia in the bronchioles.[31] While other cytokines, such CCL17 and CXCL1, may drive the initial acute inflammatory response after administration in HDM, the main drivers of persistent inflammation in the lungs are the Th2 cytokines, IL-4, IL-5, and IL-13, that appear in the lung and BALF of HDM-treated mice.[31] The canonical cells producing these cytokines include $CD4^+$ Th2 cells, eosinophils, basophils, type 2 innate lymphoid cells, and mast cells. The contribution of each of the Th2 high cytokines has been extensively studied in mouse models of asthma and in human disease and shown to induce Th2 inflammation and lung remodeling in the absence of eosinophils.[32] IL-4, largely recognized as the main driver, promotes eosinophilia, goblet cell metaplasia, airway hyperresponsiveness, IgE production, macrophage activation, smooth muscle remodeling, Th2 induction and maintenance, and subepithelial fibrosis. IL-5 is critical for stimulating eosinophil development, survival, activation and response to eotaxins.[33] IL-13 can independently induce mucus production and airway hyperresponsiveness without eosinophilia,[34] and both IL-4 and IL-13 will also drive endothelial cell production of chemokines for monocyte and macrophages and induce cell adhesion on primary human lung endothelial cells.[32]

At baseline with saline administration, the increase in IL-13 in the BALF suggests that *Hem1KO* mice may be primed or predisposed to airway hyperreactivity and goblet cell hyperplasia. Within the BALF of our HDM-treated *Hem1KO* mice, there were similar levels of IL-4, IL-5, and IL-13 as well as eotaxin (chemokine for eosinophil migration), indicating a similar Th2-high cytokine response as in the control mice. As shown via stimulation of $CD4^+$ T cells in vitro, *Hem1* deficient mice produced significantly elevated IL-13 and IL-9 (critical for mast cell growth and activation) as well as Rantes, MIP-1b, MIP-2, and MCP-1, all pro-inflammatory mediators associated with leukocyte recruitment and airway inflammation.[35–37] We suspect that despite the overall decrease in eosinophils in the airways and the lung parenchyma, $CD4^+$ Th2 cells that were similar in number in both

tissue compartments are producing exaggerated levels of Th2 and pro-inflammatory cytokines in our *Hem1KO* mice. Additionally, significant elevations in IgE in the *Hem1KO* BALF likely contribute to increased mast cell activation and degranulation, producing prostaglandins, leukotrienes, and specifically IL-13.[20]

Though there is a clear Th2 immune response in our *Hem1KO* mice, there is also evidence of a pre-existing Th17 response as noted by the elevation in IL-17 in the BALF of our saline-administered and HDM-administered mice. Based on our in vitro $CD4^+$ T cell stimulation, *Hem1* deficient $CD4^+$ T cells are likely one of the immune cells responsible for this elevation though there are likely other cells, such as innate lymphoid cells and alveolar macrophages, contributing to this elevation.[38,39] Increasing investigation into asthmatic patients with severe, steroid unresponsive clinical disease has pointed to the role of IL-17 in the development of neutrophilic or paucigranulocytic airway inflammation.[38] Though we did not see an accompanying neutrophil influx into the lungs of our *Hem1KO* mice (likely due to defective migration),[6] IL-17 is likely contributing to activation of bronchial epithelial cells and airway remodeling and fibrosis during asthma.[38]

Another interesting finding from our in vitro $CD4^+$ T cell stimulation was the significantly elevated production of IL-10 and IL-12p70 with decreased levels in VEGF (although we did not see these changes in vivo). As previously shown, allergy-limiting cytokines, such as IL-10 produced by $CD4^+IL\text{-}10^+$ cells, are also detected in BALF with HDM administration and can suppress airway hyperresponsiveness, goblet cell hyperplasia, and airway eosinophilia.[15,33] IL-10 has been shown to dampen Th2 effector cell activation and inhibit both early and late phase asthmatic responses, including mast cell activation and eosinophilic inflammation.[40] Additionally, it can inhibit IgE production while promoting IgG4 production that can be protective against allergic responses.[41] Interestingly, IL-12p70, a well-known Th1 inducer, has been considered as a possible preventative and therapeutic treatment for Th2 cell-mediated disease, such as food allergies.[42] With VEGF, elevated levels have been documented in asthmatic patients and shown to induce an asthma-like lung phenotype through IL-13 dependent and independent pathways, enhancing respiratory antigen sensitization and increasing activated dendritic cells.[16] Similar to increased levels of IL-10, decreased VEGF production from *Hem1* deficient $CD4^+$ T cells could also play a role in dampening Th2 inflammation. Further investigation into IL-10, IL-12p70, and VEGF expression in our *Hem1KO* mice in the development and progression of asthma could point towards potential treatment options for asthmatic patients.

While the HDM model provided us a comprehensive model for initial evaluation of the key players in the development of asthma in *Hem1* deficiency, we do recognize various limitations to our study. Primarily, in our *Hem1KO* mice, we were unable to perform airway

hyperresponsiveness, a standard metric to evaluate clinical severity of asthma, such as bronchoconstriction and airway sensitivity and resistance. Unfortunately, during airway testing, our *Hem1KO* mice died, and we therefore turned to histopathology as our primary metric to evaluate lung pathology. Another limitation with asthma models, specifically the HDM model, is the potential variability in asthma phenotype based on the sourced HDM lot, the method of antigen delivery, and the strain, age, and sex of the mice.[43–46] Further investigation into younger, female *Hem1KO* mice would be valuable for our understanding of the development of asthma in this population compared to adult, male mice as in this study.

Assessing the response of younger mice to HDM could also be used to further investigate IL-17 production and whether there is a change in production with age. Though we identified $CD4^+$ T cells as one possible producer of IL-17, identifying other potential sources of IL-17 production would be helpful to understand asthma pathogenesis and potential treatment modalities, such as anti-IL-17 treatment, for HEM1 deficient patients. In one paper, alveolar macrophages were actually shown to be the main producer of IL-17 in allergic airway disease in a murine ovalbumin model of asthma. Additionally, the authors demonstrated that the supernatant of OVA/IgE stimulated mast cells stimulate alveolar macrophages to increase IL-17 transcription and production, and interestingly, supernatant of OVA/DC-stimulated T cells did not induce macrophage expression of IL-17.[39] Macrophage depletion or treatment of these mice with IL-17 neutralizing antibody during OVA challenge suppressed inflammatory cell infiltration in the lungs and reduced airway hyperresponsiveness, and administration of IL-10 also effectively suppressed the increase in IL-17 producing alveolar macrophages in the OVA-challenged mice. Alternatively, we could investigate a murine model of severe neutrophilic asthma to evaluate if *Hem1KO* mice increase IL-17 production in response to this airway stimulation, or if IL-17 production remains static, suggesting a different pathway or mechanism for IL-17 production in the lungs.[47]

Another limitation that represents an area for further investigation is that our in vitro $CD4^+$ T cell stimulation was not specific to HDM antigen, which can inherently skew T cell differentiation towards a Th2 response. In vitro evaluation of HDM-antigen presentation to a naïve $CD4^+$ T cell population would demonstrate a clear immune response to HDM in our *Hem1* deficient cells. Additionally, given the decreased population of dendritic cells in the mediastinal lymph node of *Hem1KO* mice, investigating the kinetics of dendritic cell migration and allergen-specific $CD4^+$ T cell proliferation in the draining lymph node could be performed using a $Hem1^{fl/fl}CD4Cre^+$ OT-II mouse model. Use of the ovalbumin model with $Hem1^{fl/fl}CD4Cre$OT-II mice could also differentiate asthma-related airway disease from underlying baseline lung pathology. Finally, with the known link between early

childhood viral respiratory illness, such as respiratory syncytial virus or rhinovirus, and increased predisposition to develop asthma later in life, *Hem1KO* mice would be an optimal model to explore the potential link between recurring respiratory infections noted in HEM1 deficient human patients and their development of asthma.[48] Our lab has previously demonstrated poor immune response to viral and bacterial respiratory infection in conditional myeloid and B cell *Hem1* deficient mice,[7,9] and in particular, defective phagocytosis and efferocytosis shown in *Hem1* deficient alveolar macrophages likely predisposes these patients to lung inflammation and cytokine production, asthma, and autoimmunity.[49,50] Investigation of the potential mechanism of diminished efferocytosis in the development of asthma in our *Hem1KO* mice should be considered for future studies.

In conclusion, with HDM-induced asthma, *Hem1KO* mice exhibit a decreased population of eosinophils and $CD4^+$ T and B cells in various tissue compartments of the lungs. This loss of these specific immune cells in response to HDM could be driven by poor migration of myeloid cells (eosinophils and dendritic cells to the lungs or the mediastinal lymph node, respectively) and poor activation of the adaptive immune activation due to the decrease in $CD4^+$ T cells. While this decrease in immune cells could suggest a less severe asthmatic phenotype, *Hem1KO* mice instead appear to develop similar to increased pulmonary pathology and inflammation as seen on histology. This lung pathology is likely driven by both Th2 high and Th17 high cytokine production from $CD4^+$ T cells and elevated IgE production from B cells, likely leading to further activation of downstream immune cells, such as mast cells and basophils. However, conditional loss of *Hem1* in T cells or B cells alone is not sufficient to cause these changes in cell populations and cytokines, suggesting a significant role of *Hem1* deficient myeloid cells in asthma development, and likely synergistic interaction of Hem1 deficiency in many types of immune cells. Our studies reveal that loss of Hem1 plays an important role in the development of asthma and provides an opportunity to further study potential treatment modalities for asthmatic patients.

Figures

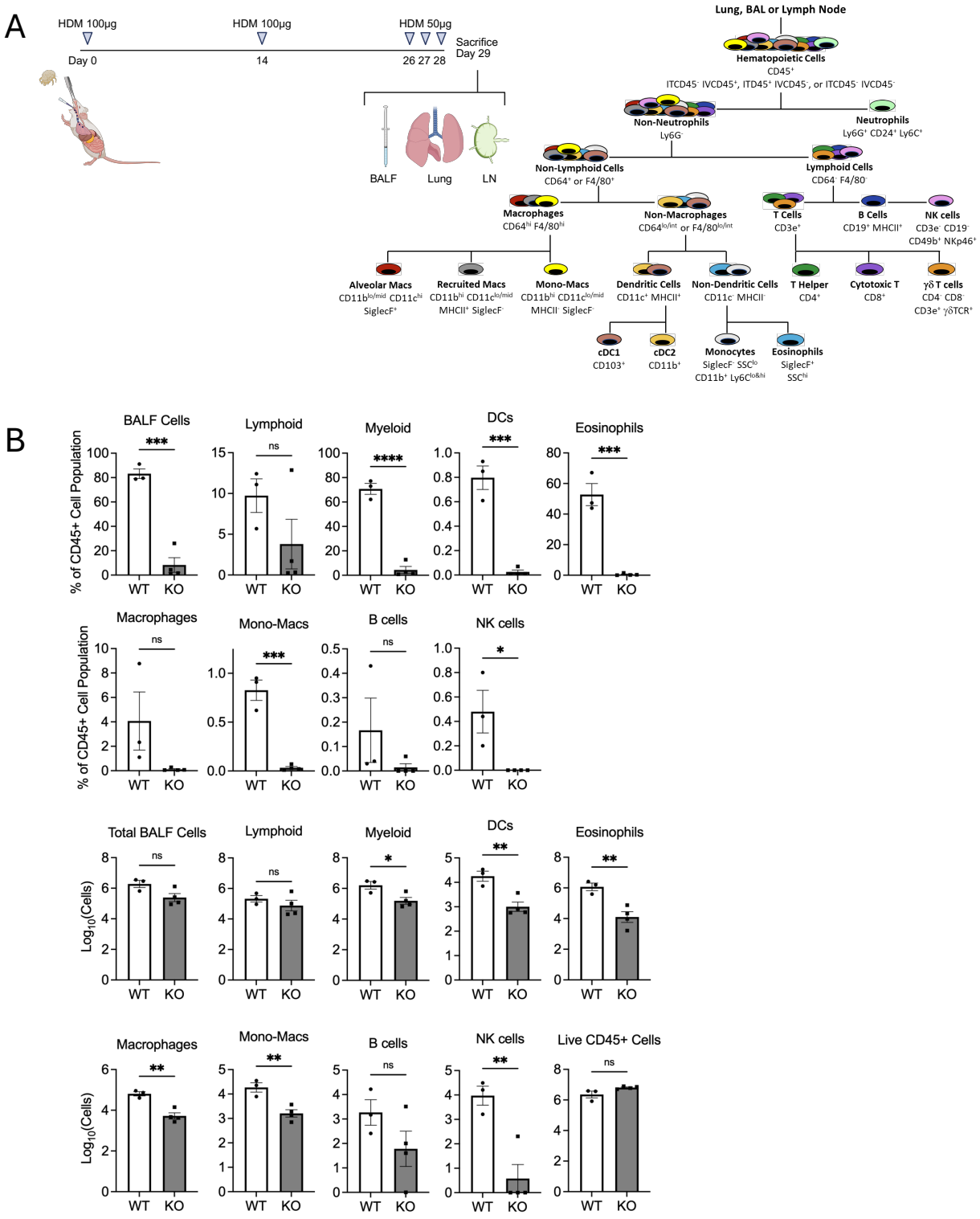

Figure 1. *Hem1KO* mice exposed to HDM have decreased myeloid cells in the bronchoalveolar lavage fluid. (Figure 1A) In part adapted from Chang et al, 2023. (A, left) Asthma regimen with administration of HDM

or saline created in BioRender. Tsai, J. (2025) https://BioRender.com/f6djx6r. *Hem1KO* mice (n=4) and littermate controls (n=3) received house dust mite via oropharyngeal administration following the timeline as shown. (A, right) As shown in Chang et al, 2023, the gating strategy for the spectral flow cytometry panel that allows for characterization of the majority of immune cells involved in the pulmonary immune response. (B) Bar graphs represent percent and total cell populations in the bronchoalveolar lavage fluid that were evaluated via spectral flow cytometry. Bar graphs represent mean ± SEM and were analyzed via unpaired Student's t test. * $p<0.05$, ** $p<0.01$, *** $p<0.001$

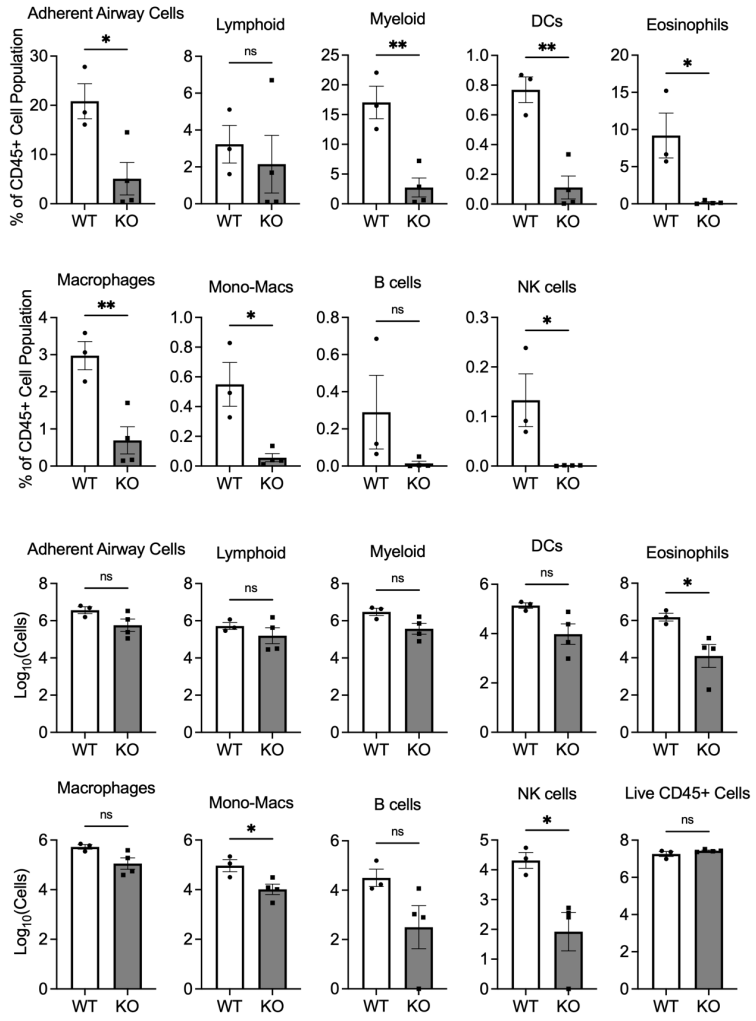

Figure 2. *Hem1KO* mice exposed to HDM have decreased myeloid cells in the adherent airways. *Hem1KO* mice (n=4) and littermate controls (n=3) received house dust mite via oropharyngeal administration following the timeline as shown. Bar graphs represent percent and total cell populations in the adherent airway that were evaluated via spectral flow cytometry. Bar graphs represent mean ± SEM and were analyzed via unpaired Student's t test. * $p<0.05$, ** $p<0.01$, *** $p<0.001$

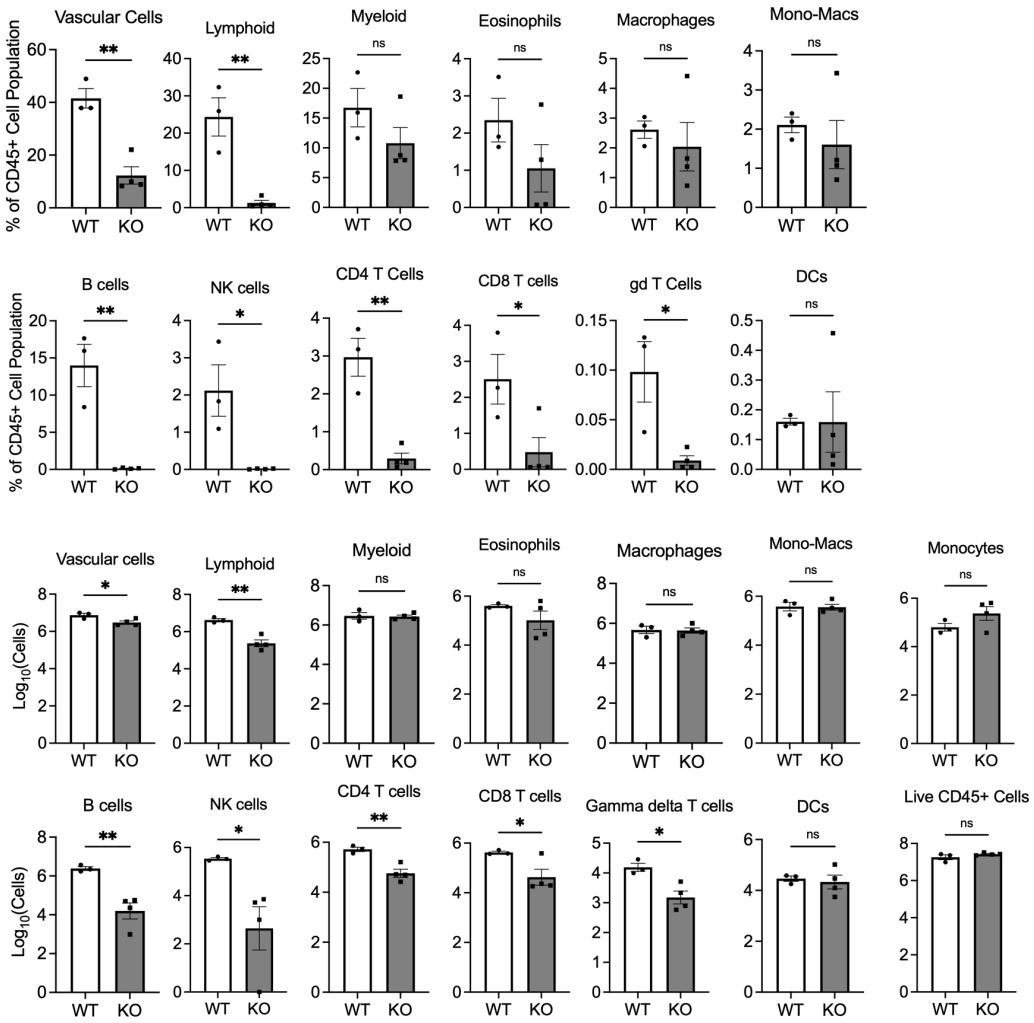

Figure 3. *Hem1KO* mice exposed to HDM have decreased lymphoid cells in the pulmonary vasculature. *Hem1KO* mice (n=4) and littermate controls (n=3) received house dust mite via oropharyngeal administration following the timeline as shown. Bar graphs represent percent and total cell populations in the lung vasculature that were evaluated via spectral flow cytometry. Bar graphs represent mean ± SEM and were analyzed via unpaired Student's t test. * $p<0.05$, ** $p<0.01$, *** $p<0.001$

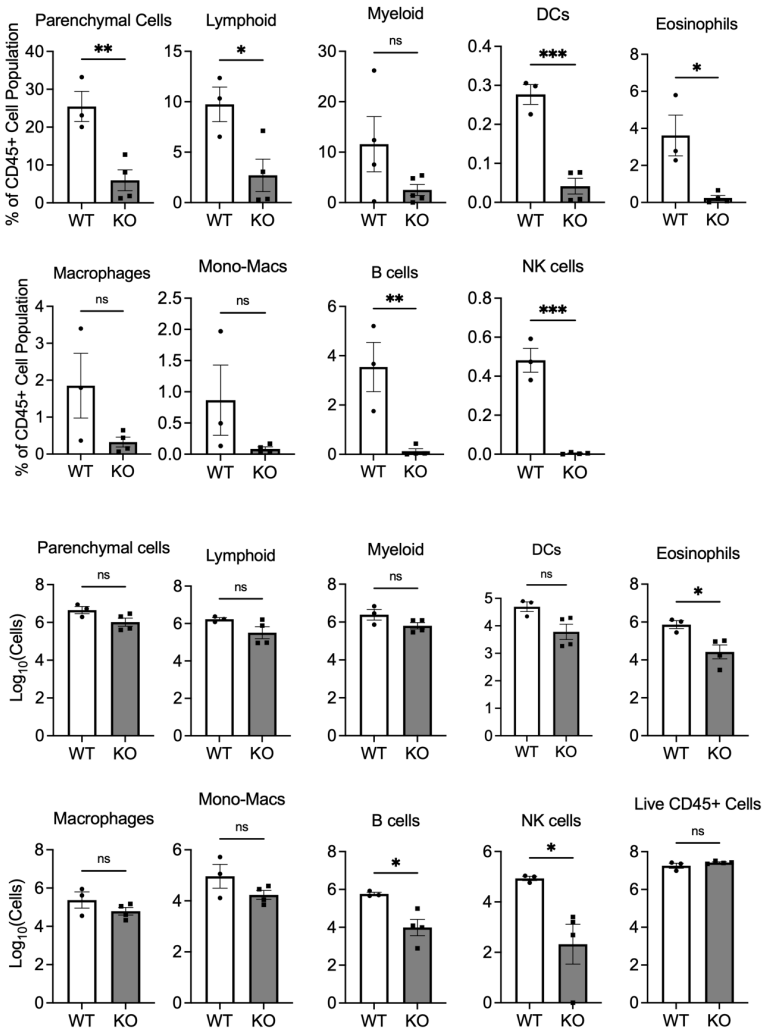

Figure 4. *Hem1KO* mice exposed to HDM have decreased eosinophils and B cells in the pulmonary interstitium. *Hem1KO* mice (n=4) and littermate controls (n=3) received house dust mite via oropharyngeal administration following the timeline as shown. Bar graphs represent percent and total cell populations in the lung interstitium that were evaluated via spectral flow cytometry. Bar graphs represent mean ± SEM and were analyzed via unpaired Student's t test. * $p<0.05$, ** $p<0.01$, *** $p<0.001$

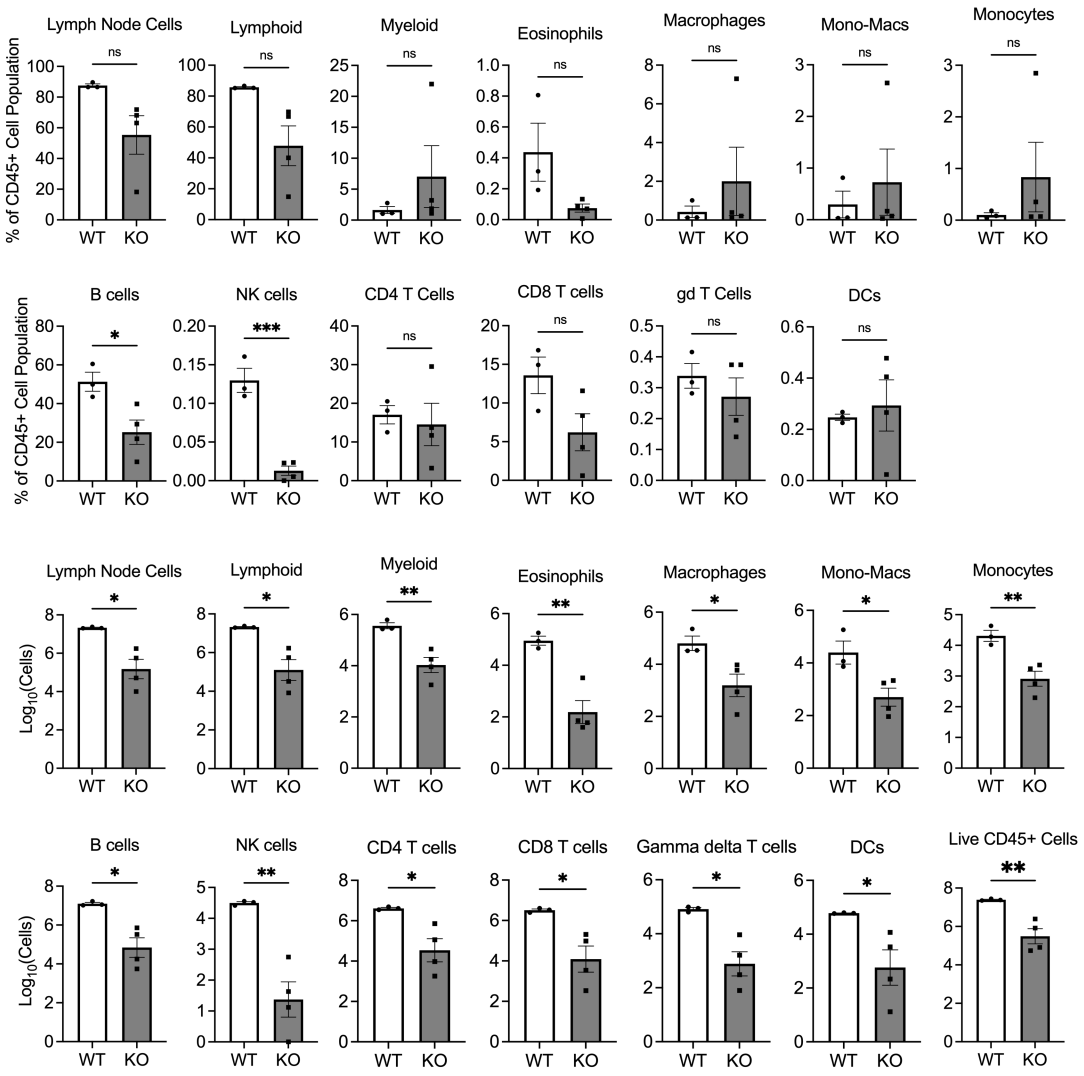

Figure 5. *Hem1KO* mice exposed to HDM have decreased myeloid and lymphoid cells, specifically dendritic cells and CD4⁺ T and B cells, in the mediastinal lymph node. *Hem1KO* mice (n=4) and littermate controls (n=3) received house dust mite via oropharyngeal administration following the timeline as shown. Bar graphs represent percent and total cell populations in the mediastinal lymph node that were evaluated via spectral flow cytometry. Bar graphs represent mean ± SEM and were analyzed via unpaired Student's t test. * p<0.05, ** p<0.01, *** p<0.001

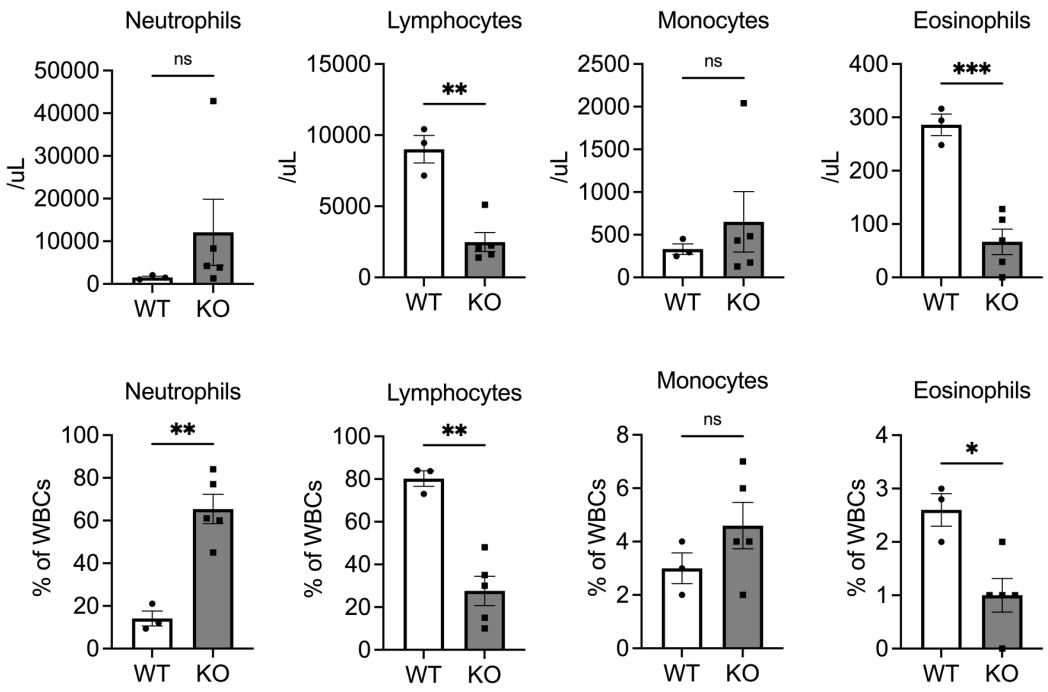

Figure 6. In the systemic circulation, *Hem1KO* mice have decreased lymphocytes and eosinophils with an increased proportion of neutrophils. Complete blood count was performed on whole blood collected via submandibular vein from *Hem1KO* (n=5) and age-matched controls (n=3). Bloodwork (cells/ul and % of WBCs) from mice at baseline with no administration of substances is shown, and bar graphs represent mean ± SEM and were analyzed via unpaired Student's t test. * $p<0.05$, ** $p<0.01$, *** $p<0.001$

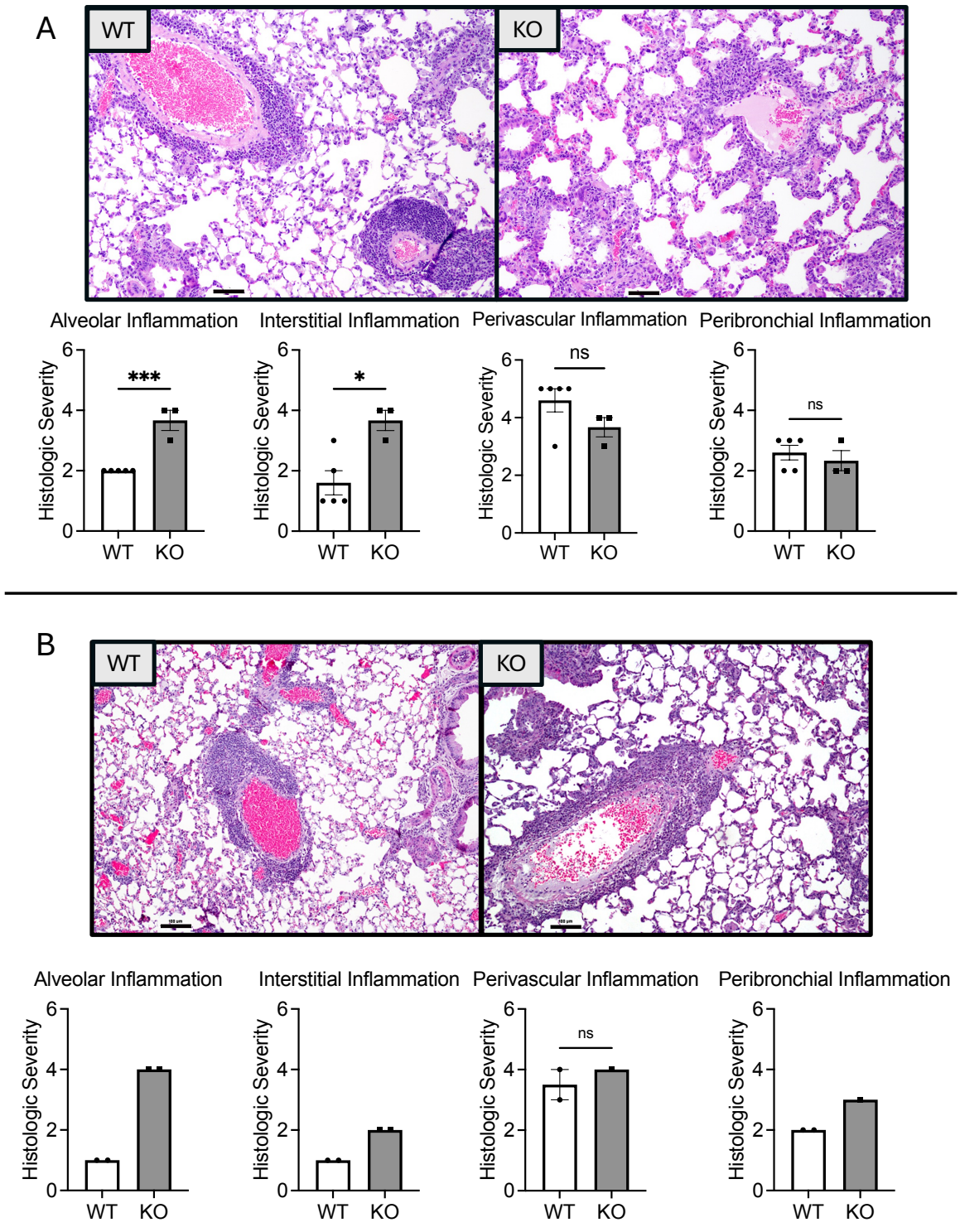

Figure 7. *Hem1KO* mice have increased alveolar and interstitial inflammation with HDM administration. Histopathologic differences between wild-type and *Hem1KO* mice that received house dust mite without concurrent administration of antibiotics (7A, n=5 for wild-type and 3 for *Hem1KO*) and with concurrent administration of antibiotics (7B, n=2/group) are shown. Slides are stained using H&E. Bar indicates 100um, 10x magnification. Bar graphs represent mean ± SEM and were analyzed via unpaired Student's t test. * $p<0.05$, ** $p<0.01$, *** $p<0.001$

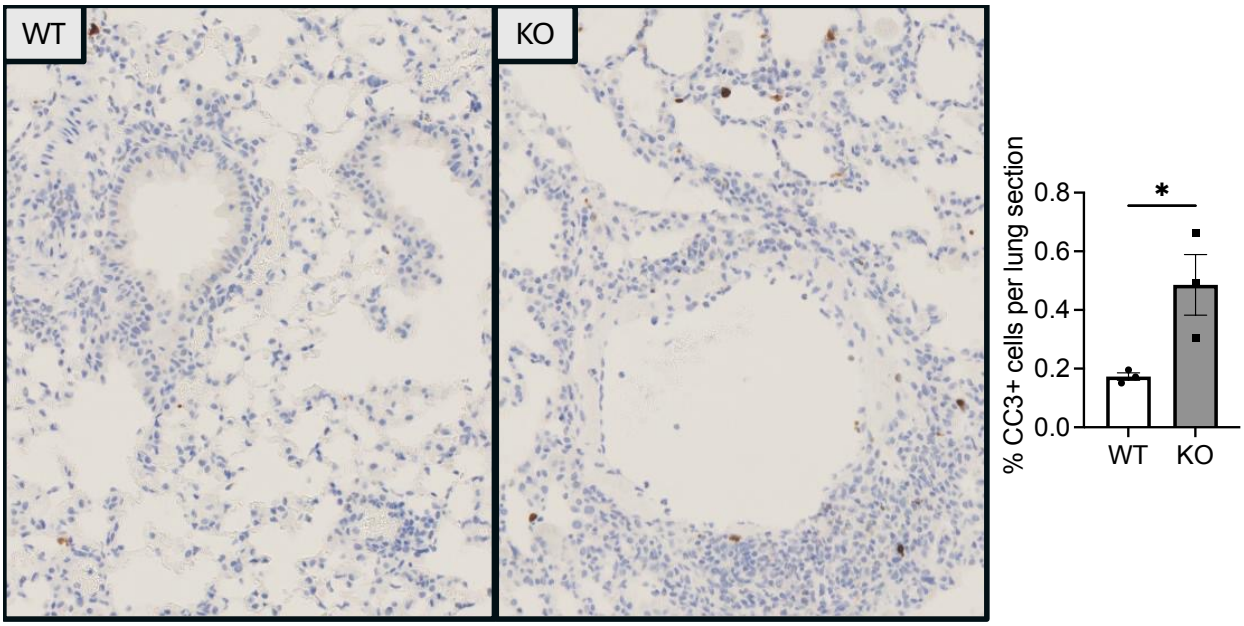

Figure 8. *Hem1KO* mice show an increased percent of apoptotic cells in the lungs with HDM administration. IHC staining of apoptotic marker cleaved caspase-3 (CC3, dilution 1:250) positive cells in lung sections of *Hem1KO* and control mice (n=3/group) after administration of HDM (magnification, 10x) are shown. Analysis of the whole-slide digital images was performed using Visiopharm software (Visiopharm, Hoersholm, Denmark). Images were processed to generate desired outputs (area of positive staining for CC3 as a ratio of positive staining to total tissue area). Bar graph shows percent of $CC3^+$ positive cells per lung section and represent mean ± SEM with analysis via unpaired Student's t test. * $p<0.05$, ** $p<0.01$, *** $p<0.001$

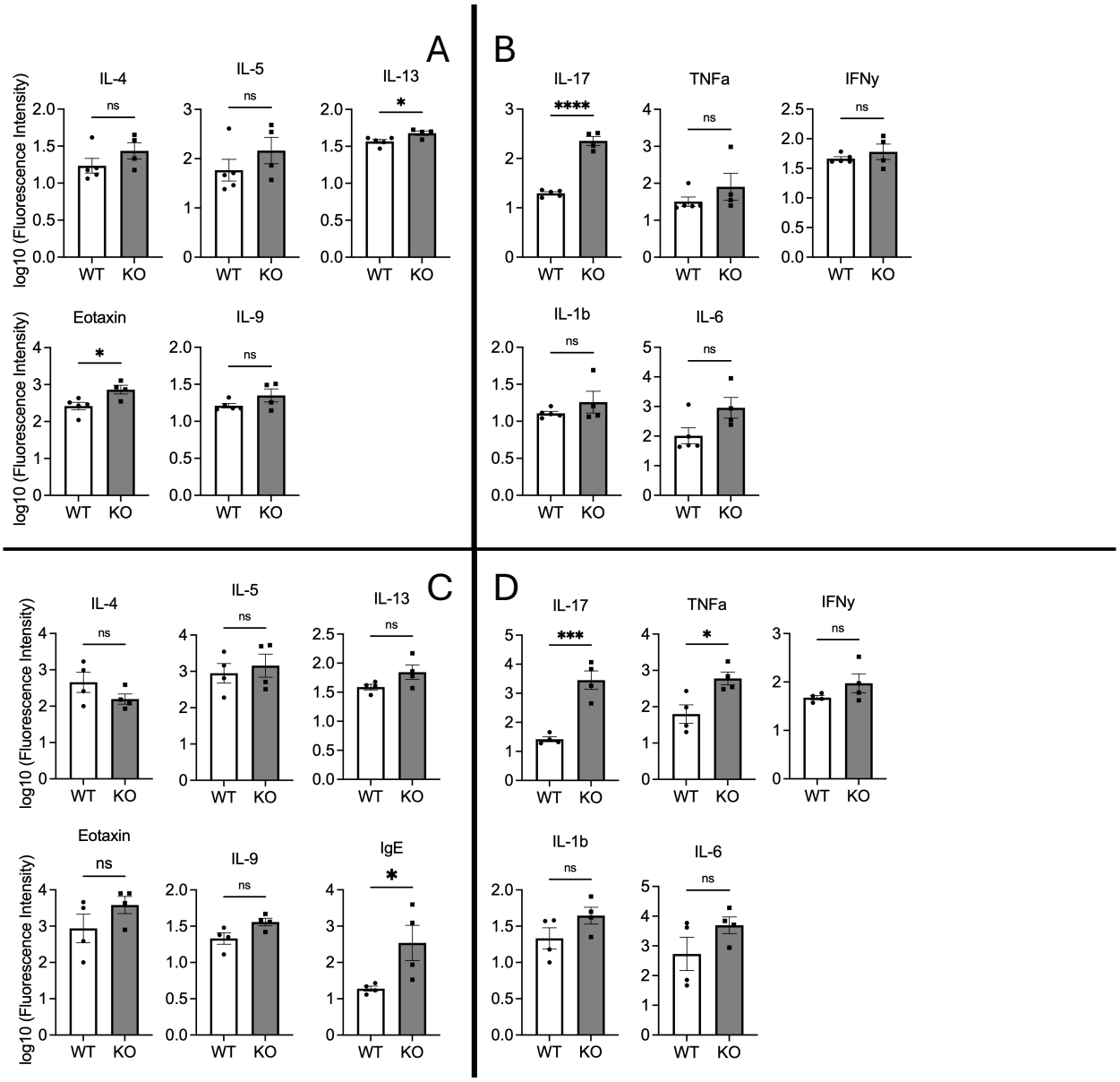

Figure 9. *Hem1KO* mice show a significantly elevated Th2 and Th17 cytokine response at baseline with saline administration and maintain an elevated Th17 cytokine response with HDM compared to controls. Bronchoalveolar lavage fluid supernatant was collected from the same mice that received saline (n=4/group) or HDM (n=4/group), and cytokine concentrations were evaluated by Eve technologies. Of the cytokines that represent the Th2 high asthma endotype (9A), IL-13 and eotaxin were elevated in our *Hem1KO* mice at baseline with saline administration. Of the cytokines characterizing a Th2 low asthma endotype (9B), IL-17 was significantly elevated. With HDM administration, Th2 high cytokine levels were similar between our *Hem1KO* and control mice; however, *Hem1KO* mice had significantly elevated IgE levels (9C). For Th2 low cytokines (9D), *Hem1KO* mice had significantly elevated IL-17 and TNFα levels compared to control mice. Bar graphs represent mean ± SEM and were analyzed via unpaired Student's t test. * $p<0.05$, ** $p<0.01$, *** $p<0.001$

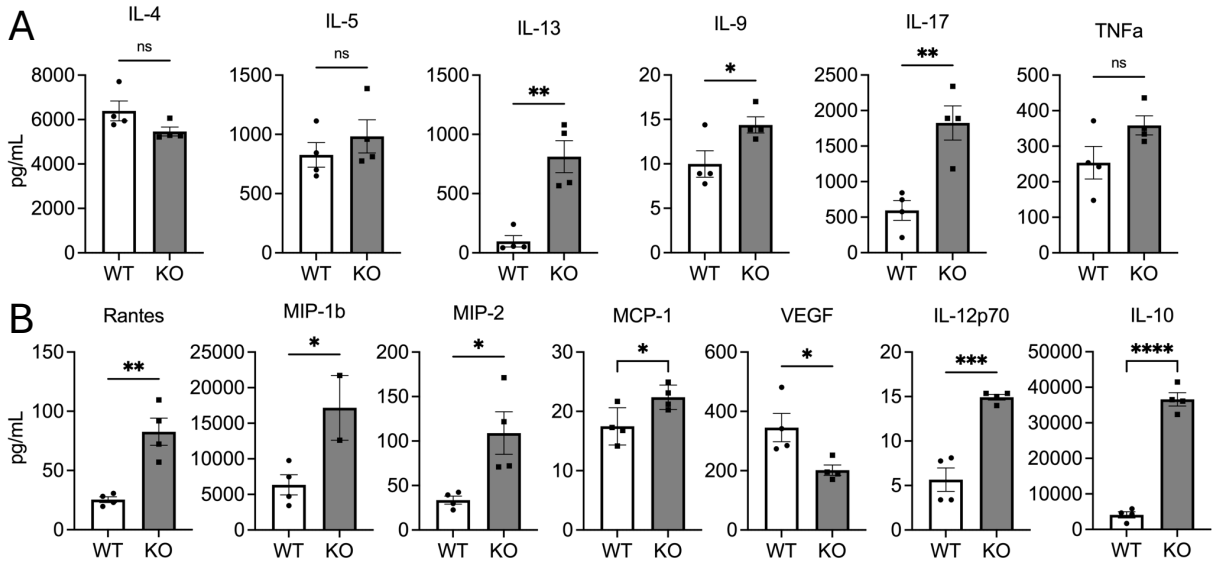

Figure 10. Isolated *Hem1* deficient CD4⁺ T cells produce elevated pro-inflammatory Th2 and Th17 cytokines upon stimulation. Purified CD4⁺ T cells from splenocytes harvested from *Hem1*$^{fl/fl}$*CD4cre*$^{+}$ mice and littermate controls (n=4/group) were stimulated with anti-CD3 and anti-CD28 antibodies for 72 hours. Bar graphs represent concentrations of cytokines in supernatant measured by multiplex immunoassay. Primary asthma cytokines are shown in (A) and other cytokines implicated in the pathogenesis of asthma are shown in (B). Bar graphs represent mean ± SEM and were analyzed via unpaired Student's t test. * $p<0.05$, ** $p<0.01$, *** $p<0.001$

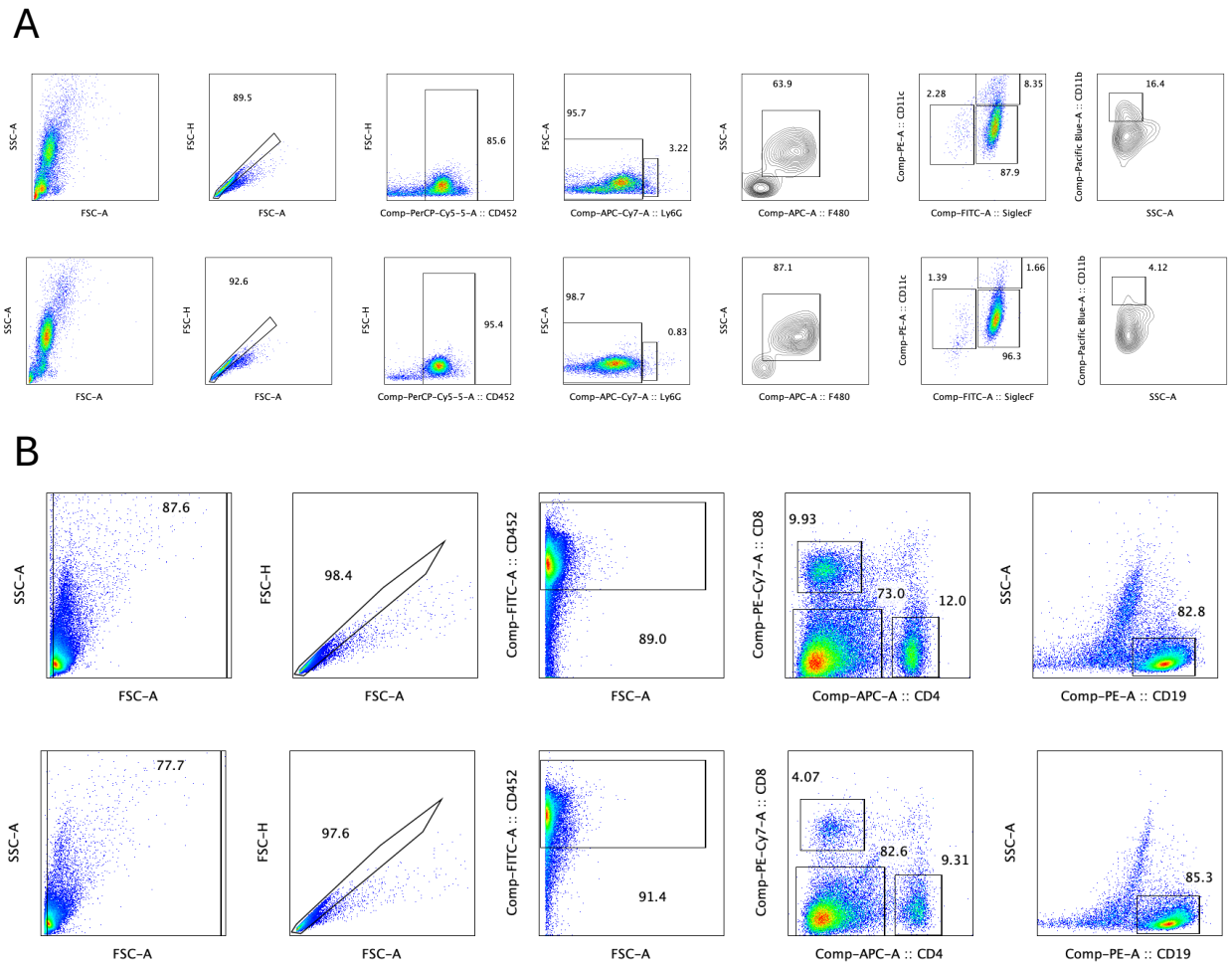

Supplemental Figure 1. Gating strategy for myeloid cells (1A) and lymphoid cells (1B) of the bronchoalveolar lavage fluid and the mediastinal lymph node in *Hem1*$^{fl/fl}$*CD4Cre*$^{+}$ and *Hem1*$^{fl/fl}$*Mb1Cre*$^{+}$ cohorts.

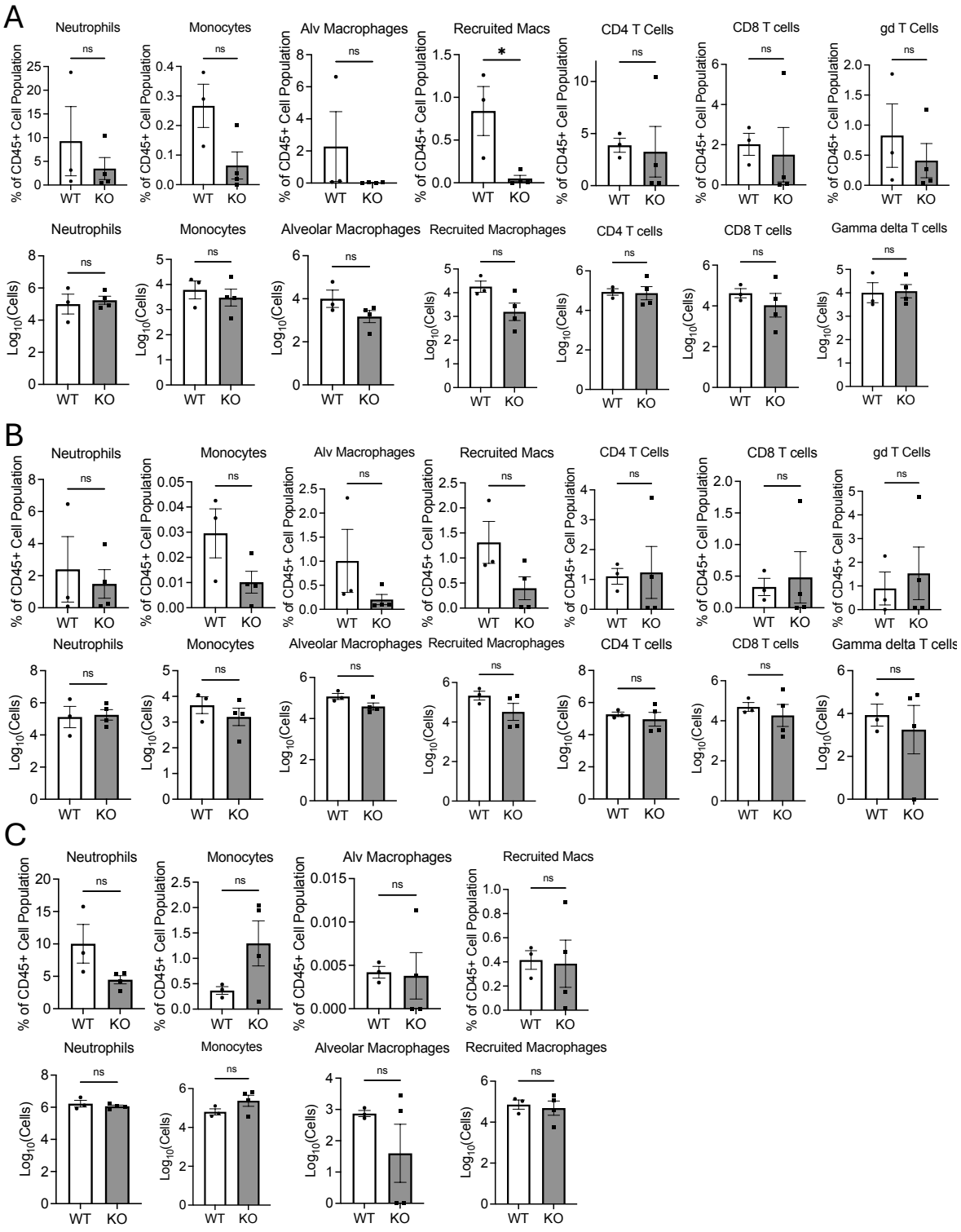

Supplemental Figure 2. Wild-type and *Hem1KO* mice received house dust mite via oropharyngeal administration following timeline as shown. Cell populations in the bronchoalveolar lavage fluid (A), adherent airway (B), and lung vasculature (C) were evaluated via flow cytometry. Bar graphs represent mean ± SEM and were analyzed via unpaired Student's t test. * $p<0.05$, ** $p<0.01$, *** $p<0.001$

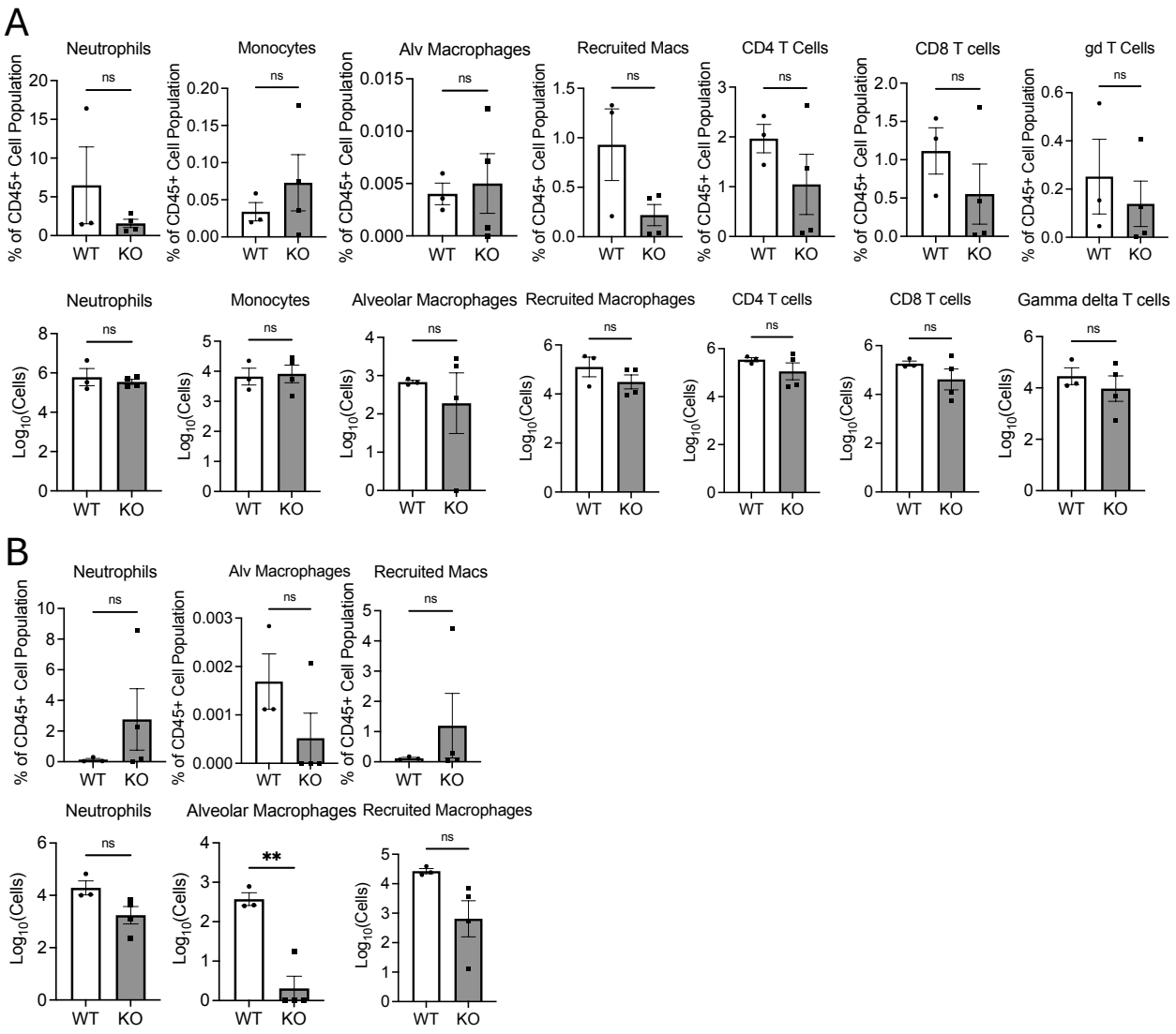

Supplemental Figure 3. Wild-type and *Hem1KO* mice received house dust mite via oropharyngeal administration following timeline as shown. Cell populations in the lung parenchyma (A) and mediastinal lymph node (B) were evaluated via flow cytometry. Bar graphs represent mean ± SEM and were analyzed via unpaired Student's t test. * $p<0.05$, ** $p<0.01$, *** $p<0.001$

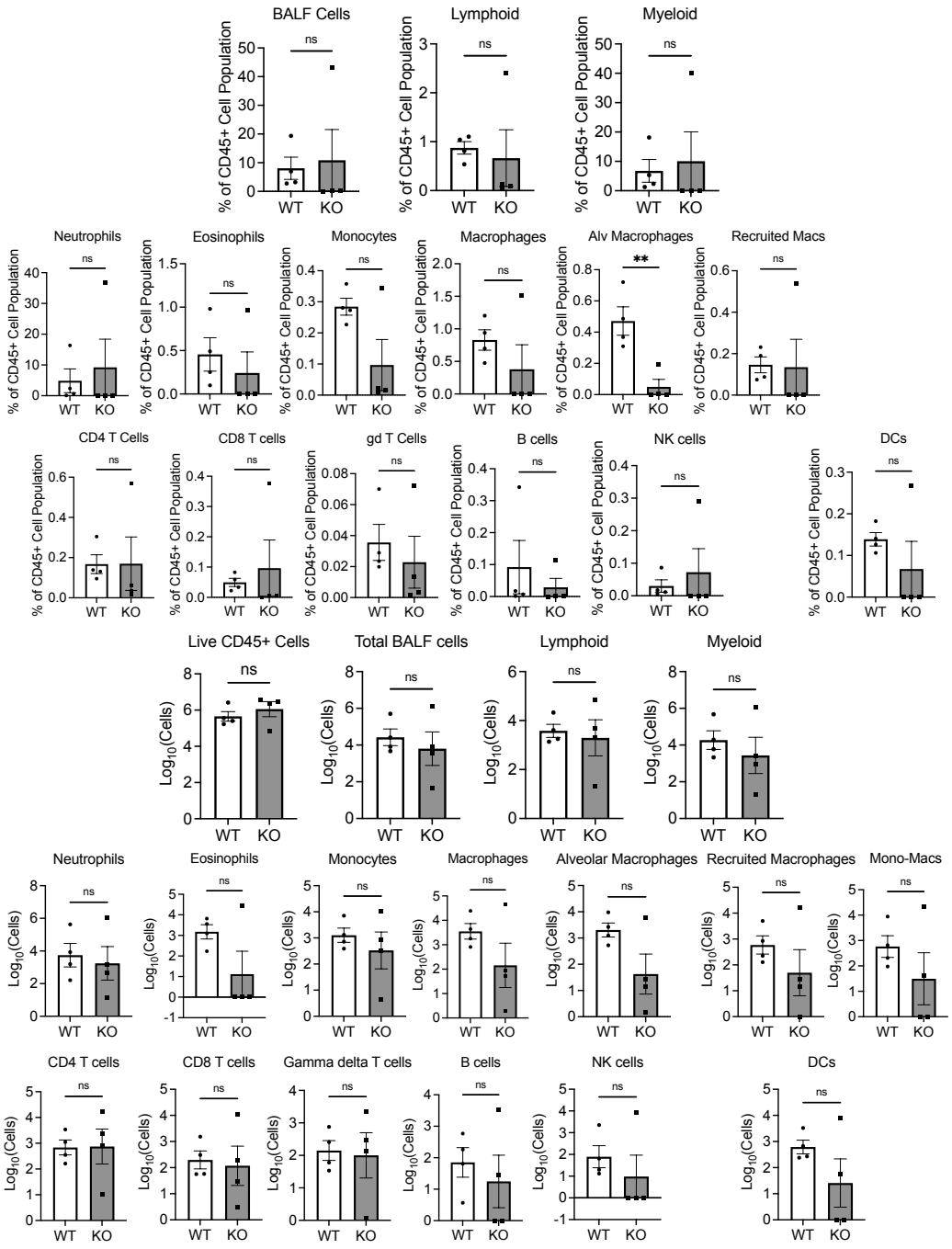

Supplemental Figure 4. Wild-type and *Hem1KO* mice received saline via oropharyngeal administration following the timeline in Figure 1 as shown. Cell populations in the bronchoalveolar lavage fluid were evaluated via flow cytometry. Bar graphs represent mean ± SEM and were analyzed via unpaired Student's t test. * $p<0.05$, ** $p<0.01$, *** $p<0.001$

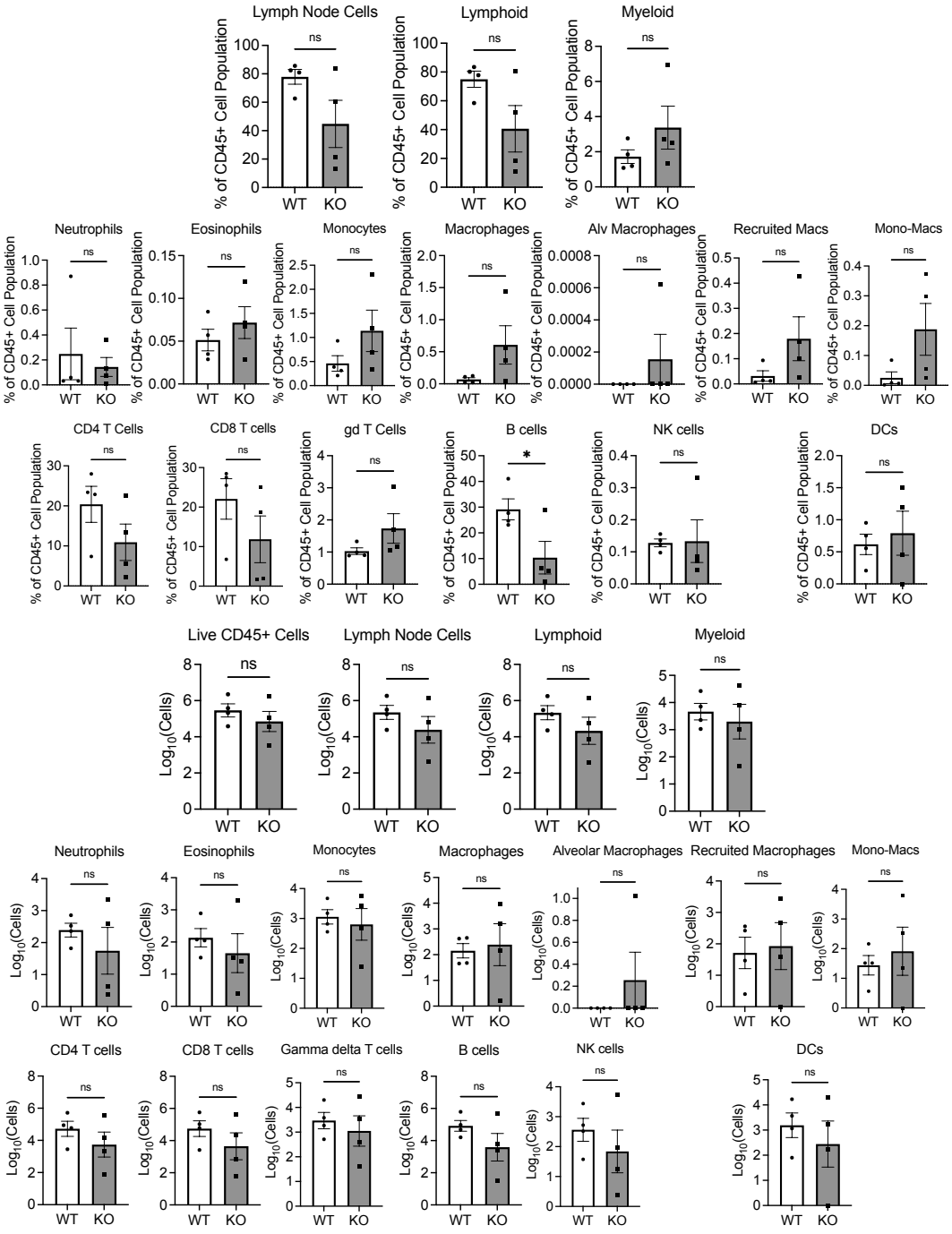

Supplemental Figure 5. Wild-type and *Hem1KO* mice received saline via oropharyngeal administration following the timeline in Figure 1 as shown. Cell populations in the mediastinal lymph node were evaluated via flow cytometry. Bar graphs represent mean ± SEM and were analyzed via unpaired Student's t test. * p<0.05, ** p<0.01, *** p<0.001

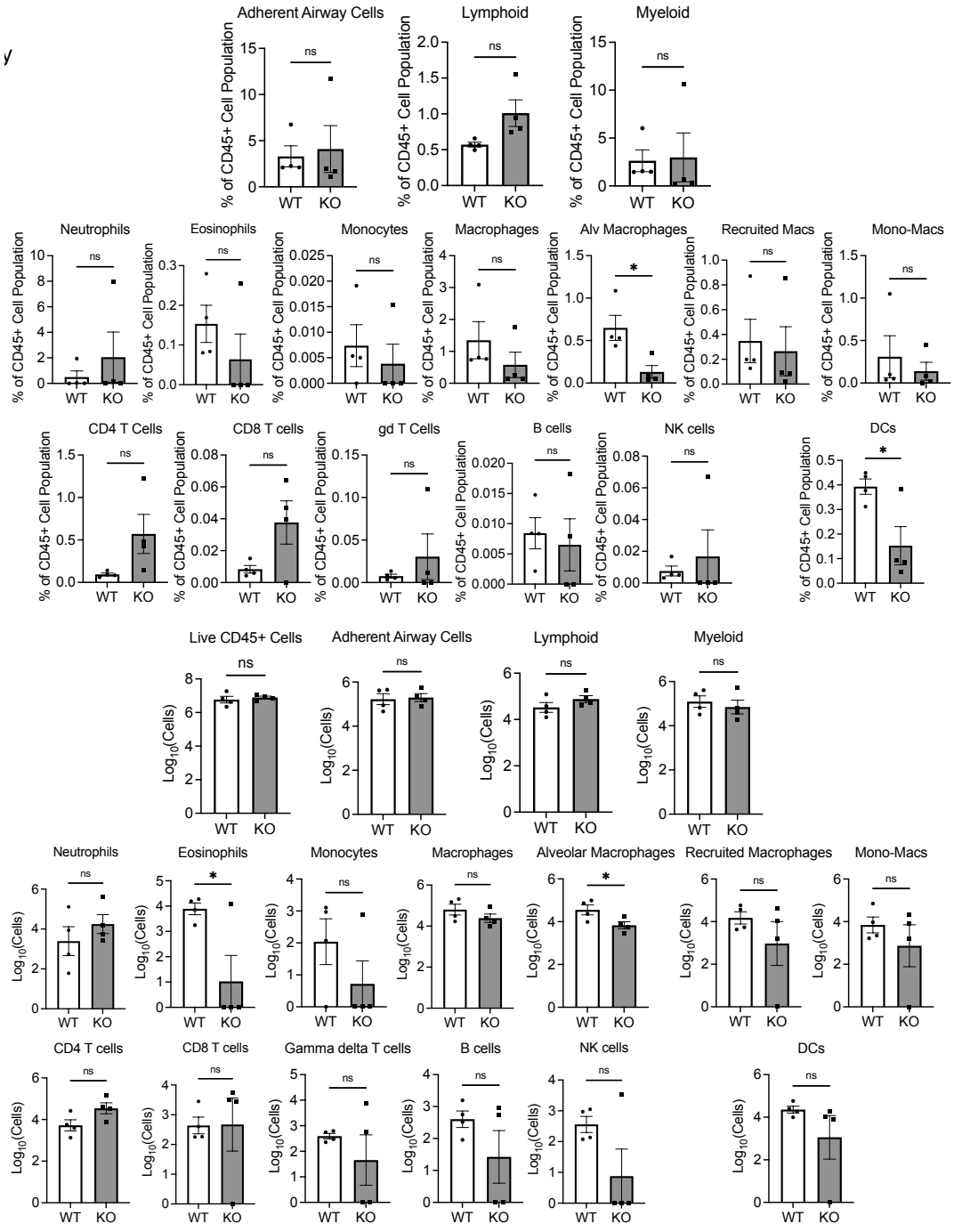

Supplemental Figure 6. Wild-type and *Hem1KO* mice received saline via oropharyngeal administration following the timeline in Figure 1 as shown. Cell populations in the lung airways were evaluated via flow cytometry. Bar graphs represent mean ± SEM and were analyzed via unpaired Student's t test. * p<0.05, ** p<0.01, *** p<0.001

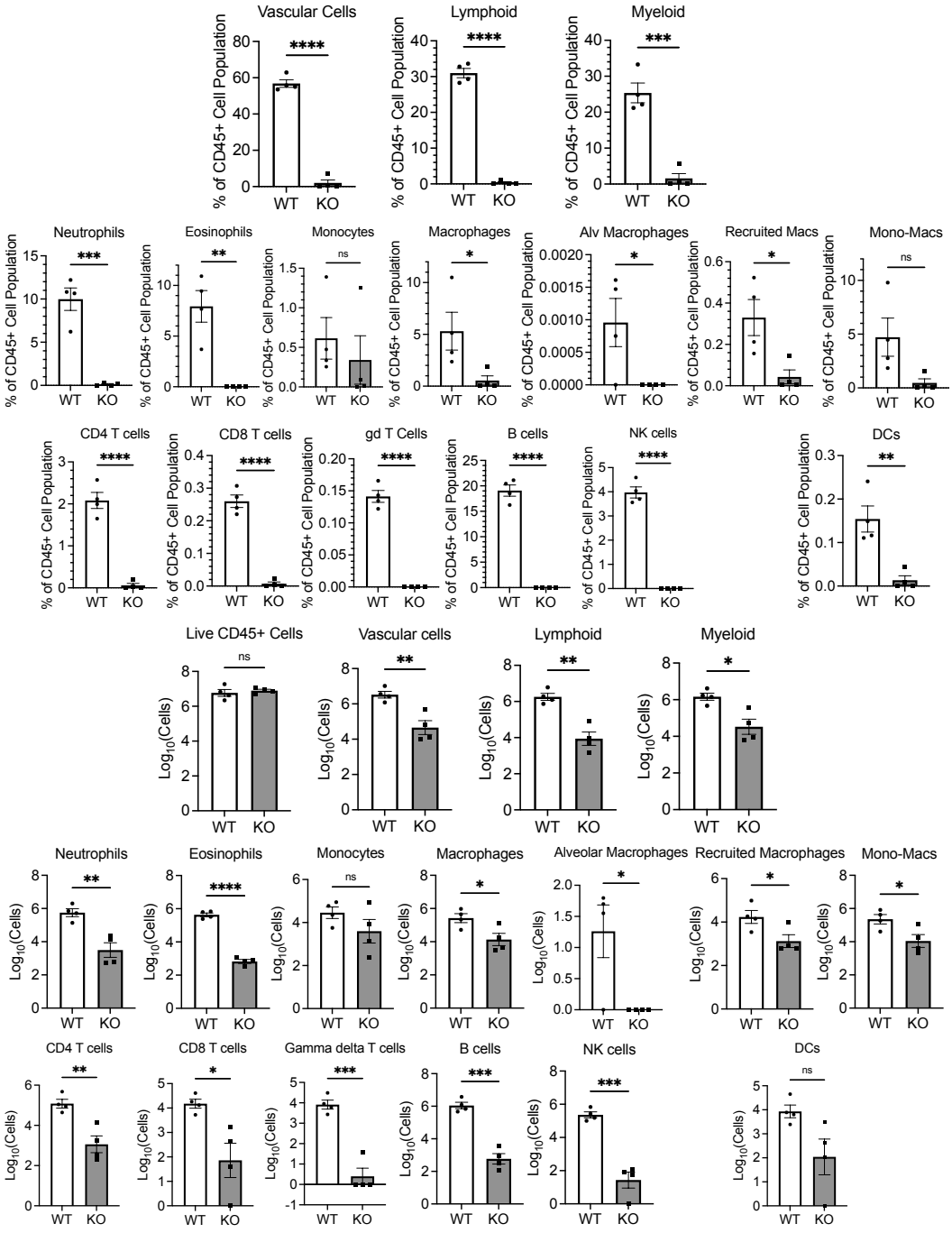

Supplemental Figure 7. Wild-type and *Hem1KO* mice received saline via oropharyngeal administration following the timeline in Figure 1 as shown. Cell populations in the lung vasculature were evaluated via flow cytometry. Bar graphs represent mean ± SEM and were analyzed via unpaired Student's t test. * $p<0.05$, ** $p<0.01$, *** $p<0.001$

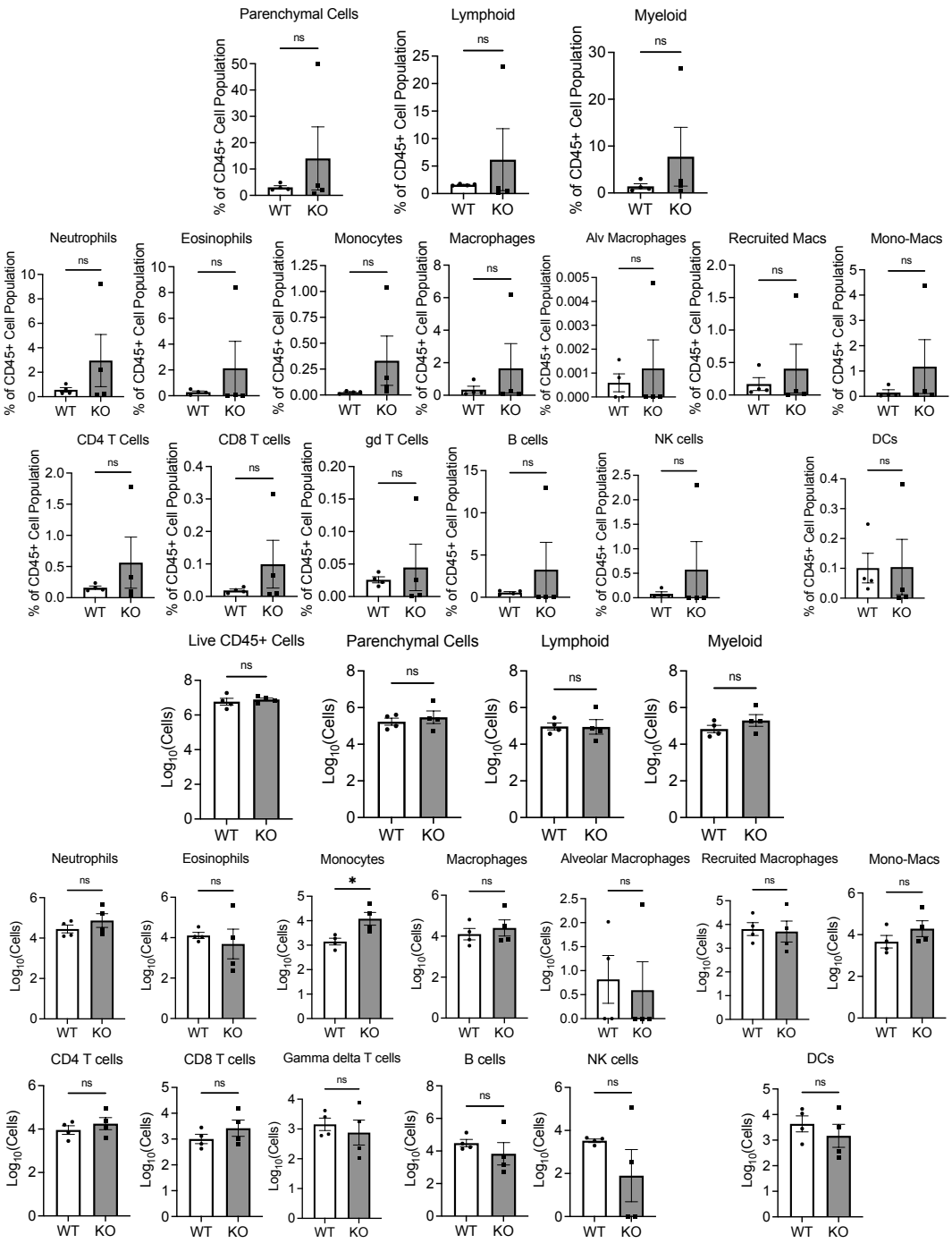

Supplemental Figure 8. Wild-type and *Hem1KO* mice received saline via oropharyngeal administration following the timeline in Figure 1 as shown. Cell populations in the lung interstitium were evaluated via flow cytometry. Bar graphs represent mean ± SEM and were analyzed via unpaired Student's t test. * p<0.05, ** p<0.01, *** p<0.001

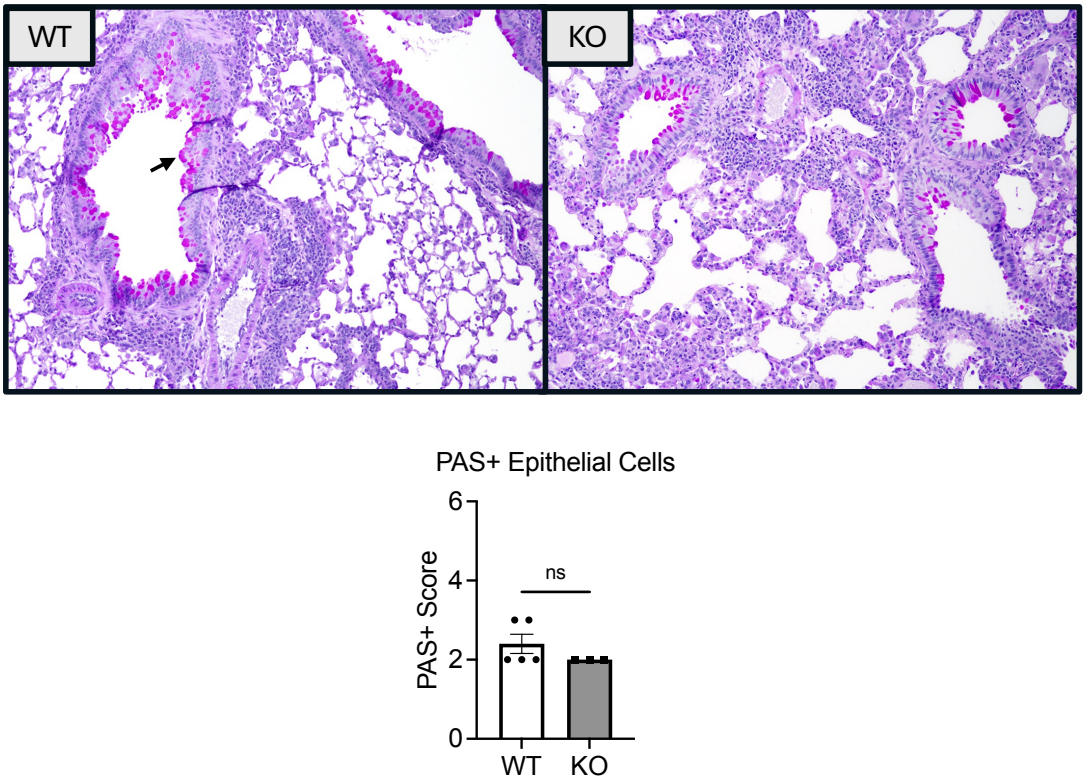

Supplementary Figure 9. Lung sections from Hem1KO and control mice that received HDM were stained with PAS (magnification 10x, positive epithelial bronchiole cell indicated by the black arrow). Data for mice that received antibiotics with HDM not shown. PAS-stained sections were scored from 0-4, reflecting <5%, 5-25%, 25-50%, 50-75%, and >75% mucus positive epithelial cells per bronchiole, respectively. Bar graphs represent mean ± SEM and were analyzed via unpaired Student's t test. * $p<0.05$, ** $p<0.01$, *** $p<0.001$

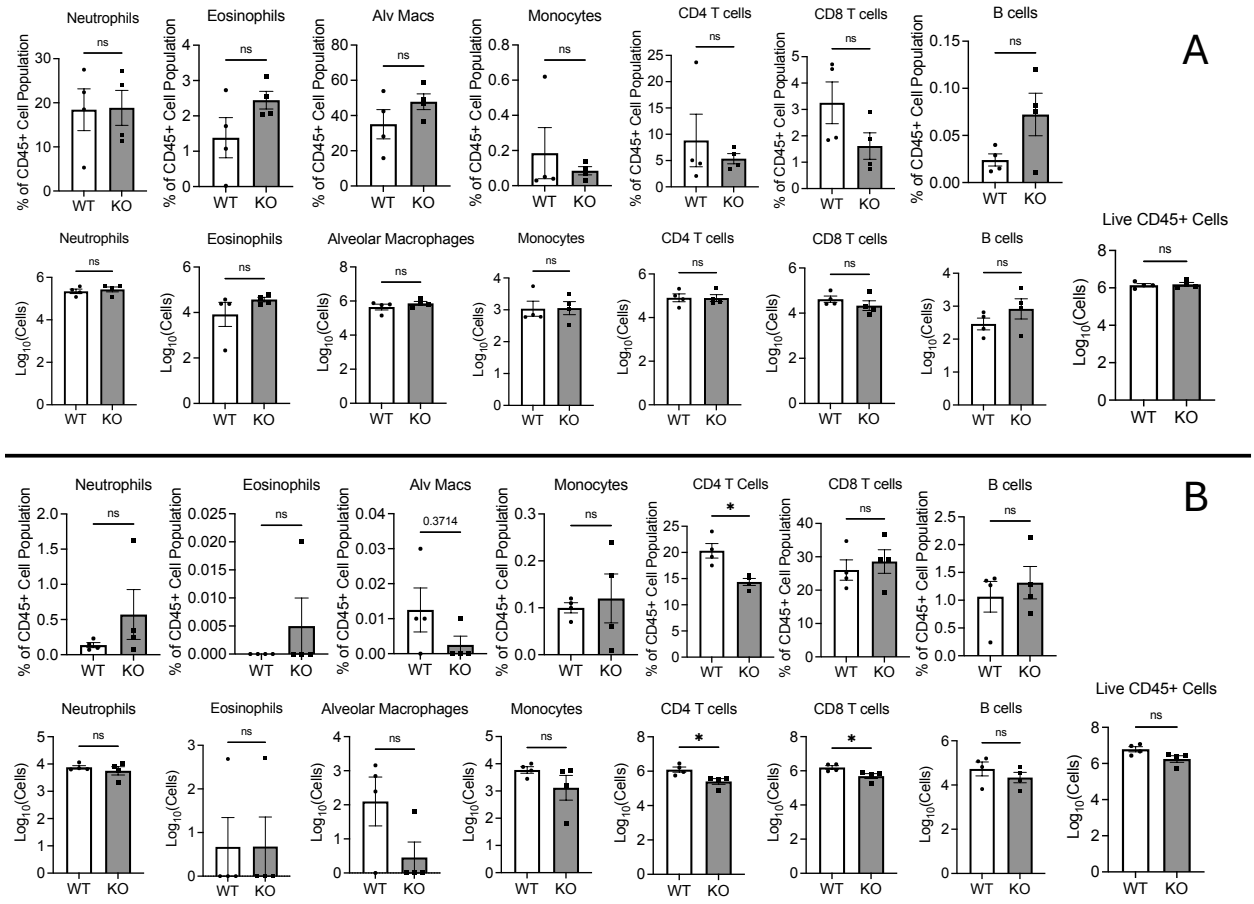

Supplemental Figure 10. Wild-type and *Hem1*$^{fl/fl}$*CD4Cre*$^{+}$ mice received saline via oropharyngeal administration following timeline as shown. Percent and total cell populations in the bronchoalveolar lavage fluid (A) and mediastinal lymph node (B) were evaluated via flow cytometry. Bar graphs represent mean ± SEM and were analyzed via unpaired Student's t test. * p<0.05, ** p<0.01, *** p<0.001

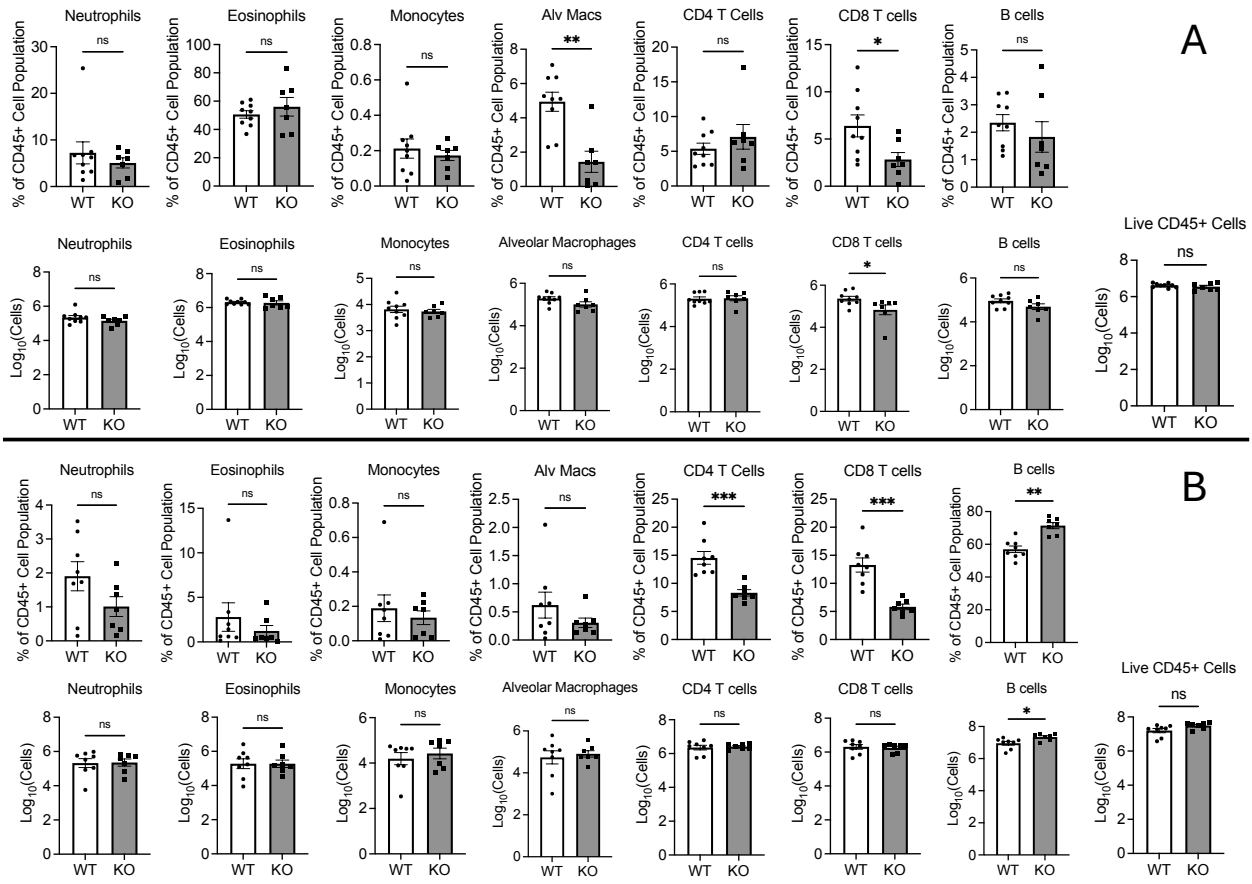

Supplemental Figure 11. Wild-type and *Hem1*$^{fl/fl}$*CD4Cre*$^{+}$ mice received house dust mite via oropharyngeal administration following timeline as shown. Percent and total cell populations in the bronchoalveolar lavage fluid (A) and mediastinal lymph node (B) were evaluated via flow cytometry. Bar graphs represent mean ± SEM and were analyzed via unpaired Student's t test. * $p<0.05$, ** $p<0.01$, *** $p<0.001$

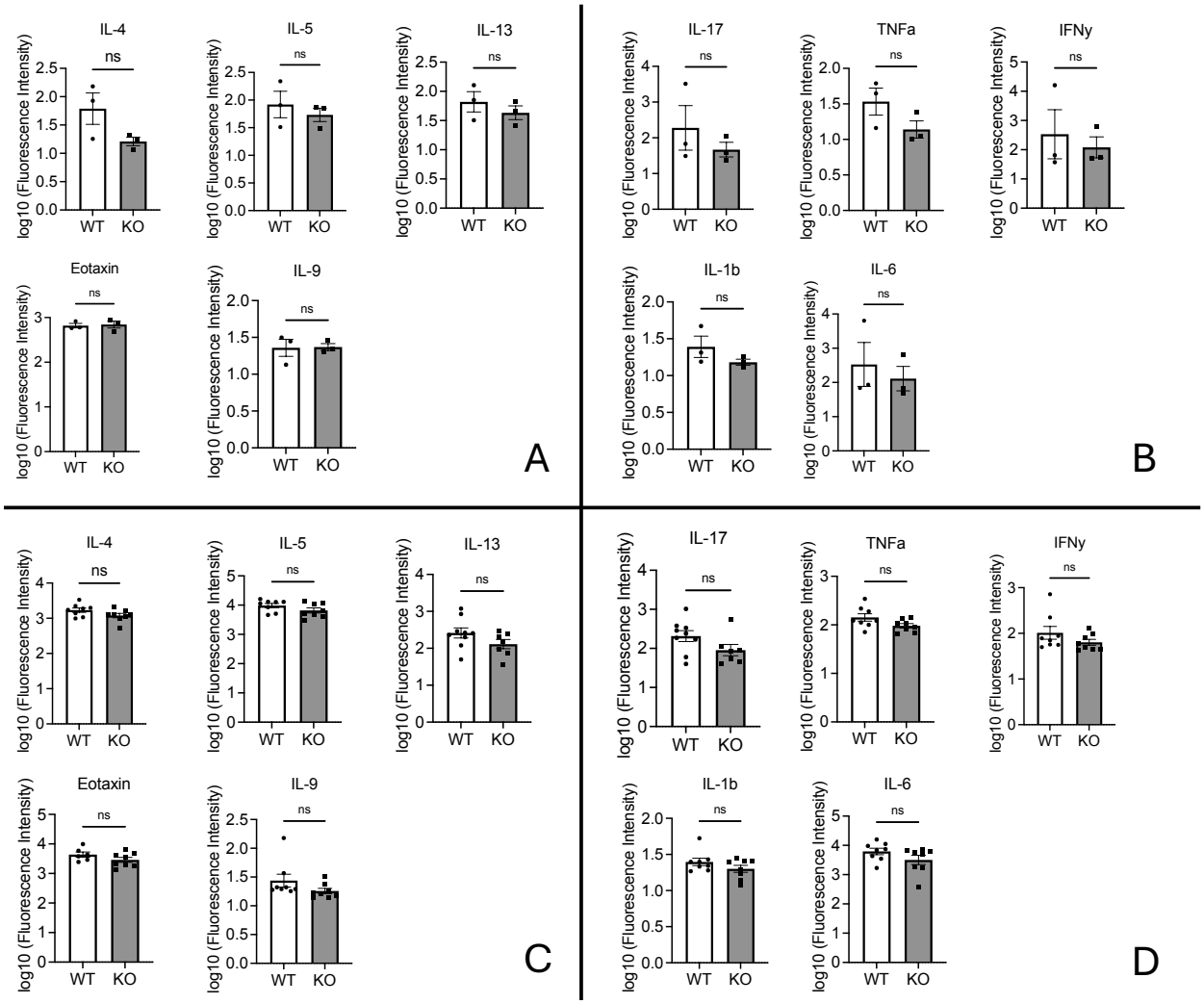

Supplemental Figure 12. Bronchoalveolar lavage fluid supernatant was collected from the mice in Supplemental Fig 10 and 11, and cytokine levels were evaluated by Eve technologies (Luminex). Cytokine levels from *Hem1*$^{fl/fl}$*CD4Cre*$^{+}$ mice that received saline are shown in A and B while *Hem1*$^{fl/fl}$*CD4Cre*$^{+}$ mice that received HDM are shown in C and D. Bar graphs represent mean ± SEM and were analyzed via unpaired Student's t test. * $p<0.05$, ** $p<0.01$, *** $p<0.001$

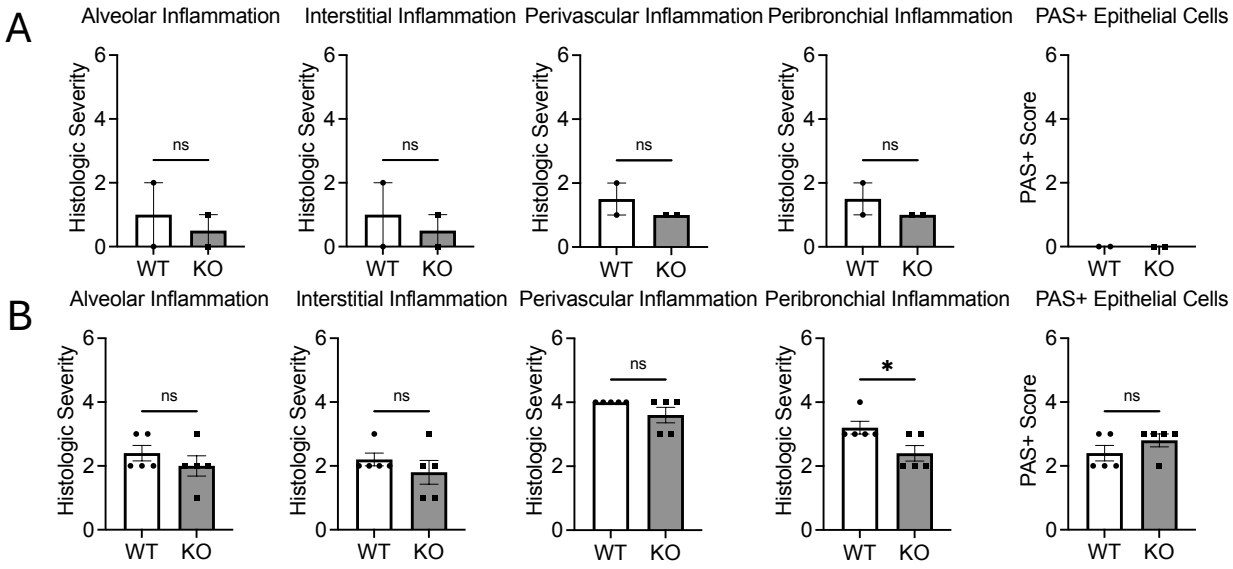

Supplemental Figure 13. Histopathology differences between wild-type and *Hem1*$^{fl/fl}$*CD4Cre*$^{+}$ mice that received saline (A) or HDM (B). PAS+ epithelial cells were not significantly different between the wild-type and *Hem1*$^{fl/fl}$*CD4Cre*$^{+}$ mice in either the saline or HDM cohorts. Bar graphs represent mean ± SEM and were analyzed via unpaired Student's t test. * p<0.05, ** p<0.01, *** p<0.001

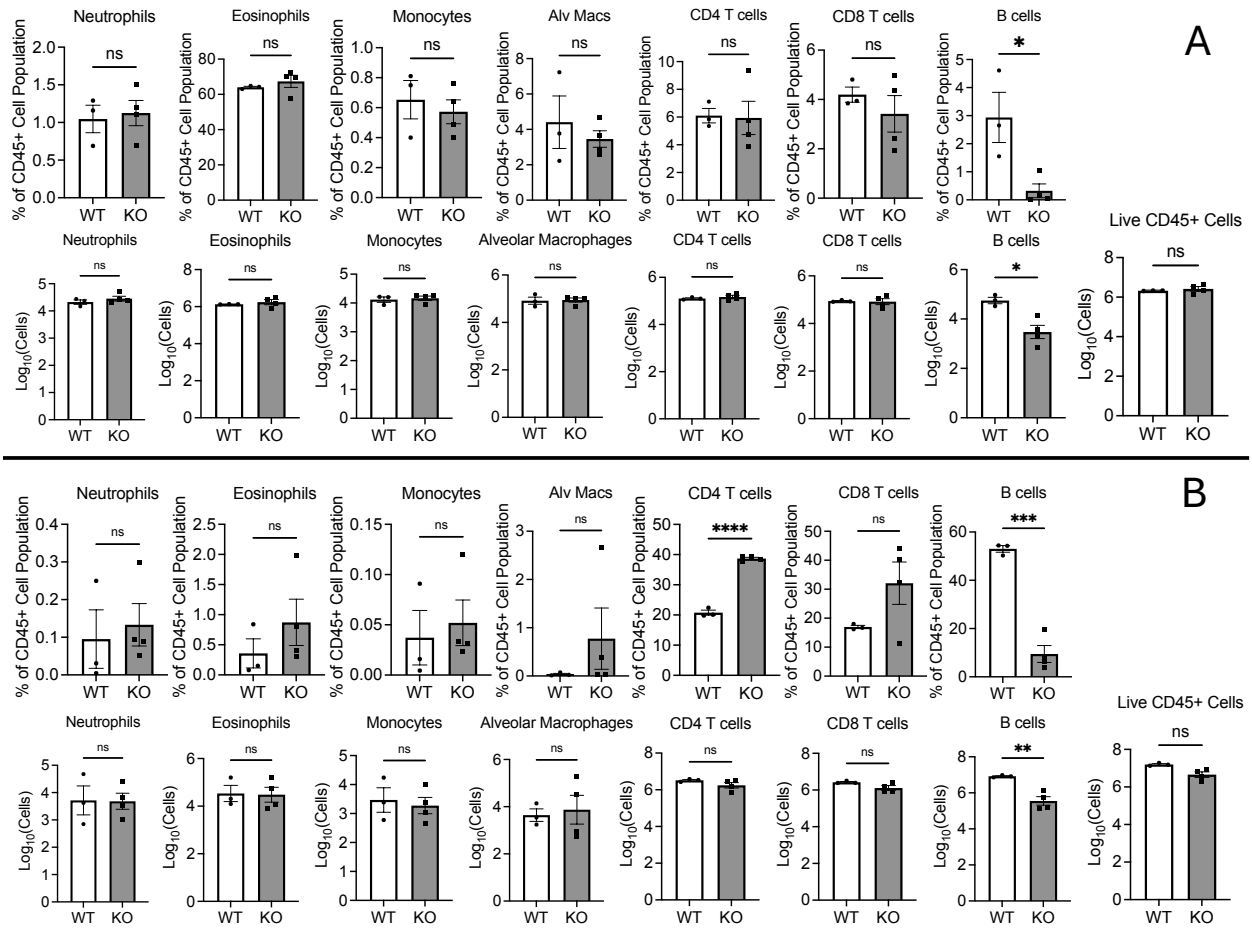

Supplemental Figure 14. Wild-type and *Hem1*$^{fl/fl}$*Mb1Cre*$^{+}$ mice received house dust mite via oropharyngeal administration following timeline as shown. Cell populations in the bronchoalveolar lavage fluid (A) and mediastinal lymph node (B) were evaluated via flow cytometry. Bar graphs represent mean ± SEM and were analyzed via unpaired Student's t test. * p<0.05, ** p<0.01, *** p<0.001

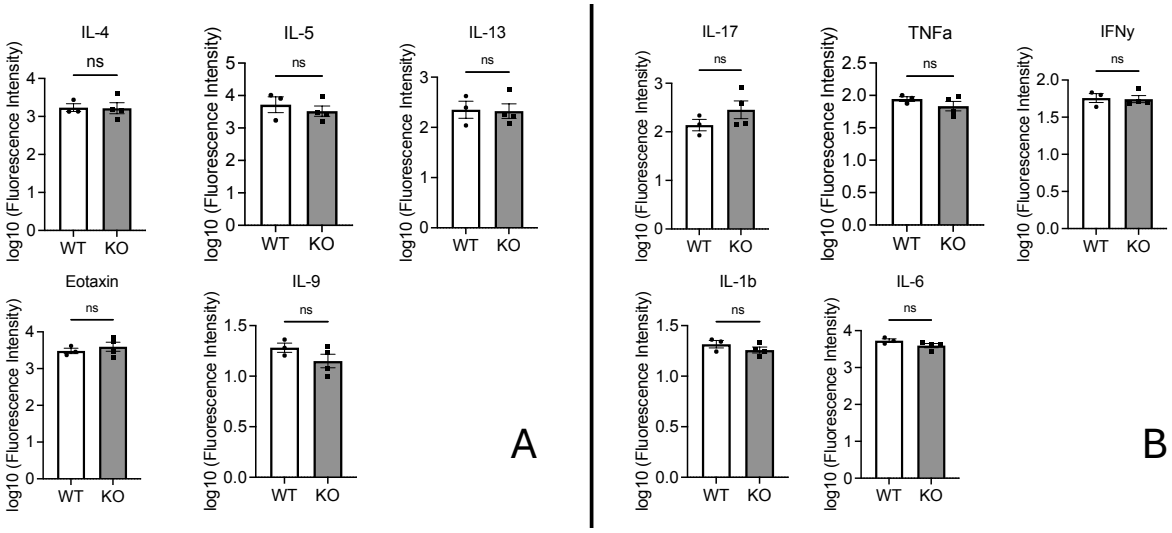

Supplemental Figure 15. Bronchoalveolar lavage fluid supernatant was collected from the *Hem1*$^{fl/fl}$*Mb1Cre*$^{+}$ mice in Supplemental Figure 14, and cytokine levels were evaluated by Eve technologies. Th2 high cytokines (A) and Th2 low cytokines (B) are shown. Bar graphs represent mean ± SEM and were analyzed via unpaired Student's t test. * $p<0.05$, ** $p<0.01$, *** $p<0.001$

References

1. Cook S, Lenardo MJ, Freeman AF. HEM1 Actin Immunodysregulatory Disorder: Genotypes, Phenotypes, and Future Directions. *J Clin Immunol*. 2022;42(8):1583-1592. doi:10.1007/s10875-022-01327-0

2. Cook SA, Comrie WA, Poli MC, et al. HEM1 deficiency disrupts mTORC2 and F-actin control in inherited immunodysregulatory disease. *Science*. 2020;369(6500):202-207. doi:10.1126/science.aay5663

3. Castro CN, Rosenzwajg M, Carapito R, et al. NCKAP1L defects lead to a novel syndrome combining immunodeficiency, lymphoproliferation, and hyperinflammation. *J Exp Med*. 2020;217(12):e20192275. doi:10.1084/jem.20192275

4. Salzer E, Zoghi S, Kiss MG, et al. The cytoskeletal regulator HEM1 governs B cell development and prevents autoimmunity. *Sci Immunol*. 2020;5(49):eabc3979. doi:10.1126/sciimmunol.abc3979

5. Christodoulou A, Tsai JY, Suwankitwat N, Anderson A, Iritani BM. Hem1 inborn errors of immunity: waving goodbye to coordinated immunity in mice and humans. *Front Immunol*. 2024;15. doi:10.3389/fimmu.2024.1402139

6. Park H, Staehling-Hampton K, Appleby MW, et al. A point mutation in the murine Hem1 gene reveals an essential role for Hematopoietic Protein 1 in lymphopoiesis and innate immunity. *J Exp Med*. 2008;205(12):2899-2913. doi:10.1084/jem.20080340

7. Avalos A, Tietsort JT, Suwankitwat N, et al. Hem-1 regulates protective humoral immunity and limits autoantibody production in a B cell–specific manner. doi:10.1172/jci.insight.153597

8. Weiner OD, Rentel MC, Ott A, et al. Hem-1 complexes are essential for Rac activation, actin polymerization, and myosin regulation during neutrophil chemotaxis. *PLoS Biol*. 2006;4(2):e38. doi:10.1371/journal.pbio.0040038

9. Suwankitwat N, Libby S, Liggitt HD, et al. The actin-regulatory protein Hem-1 is essential for alveolar macrophage development. *J Exp Med*. 2021;218(4):e20200472. doi:10.1084/jem.20200472

10. Leithner A, Altenburger LM, Hauschild R, et al. Dendritic cell actin dynamics control contact duration and priming efficiency at the immunological synapse. *J Cell Biol*. 2021;220(4). doi:10.1083/jcb.202006081

11. Leithner A, Eichner A, Müller J, et al. Diversified actin protrusions promote environmental exploration but are dispensable for locomotion of leukocytes. *Nat Cell Biol*. 2016;18(11):1253-1259. doi:10.1038/ncb3426

12. Habib N, Pasha MA, Tang DD. Current Understanding of Asthma Pathogenesis and Biomarkers. *Cells*. 2022;11(17):2764. doi:10.3390/cells11172764

13. Chang MY, Brune JE, Black M, Altemeier WA, Frevert CW. Multicompartmental analysis of the murine pulmonary immune response by spectral flow cytometry. *Am J Physiol-Lung Cell Mol Physiol*. 2023;325(4):L518-L535. doi:10.1152/ajplung.00317.2022

14. Branchett WJ, Walker SA, Lloyd CM. Experimental Mouse Models of Asthma and Analysis of CD4 T Cells. In: Annunziato F, Maggi L, Mazzoni A, eds. *T-Helper Cells: Methods and Protocols*. Methods in Molecular Biology. Springer US; 2021:329-348. doi:10.1007/978-1-0716-1311-5_25

15. Gregory LG, Causton B, Murdoch JR, et al. Inhaled house dust mite induces pulmonary T helper 2 cytokine production. *Clin Exp Allergy J Br Soc Allergy Clin Immunol*. 2009;39(10):1597-1610. doi:10.1111/j.1365-2222.2009.03302.x

16. Lee CG, Link H, Baluk P, et al. Vascular endothelial growth factor (VEGF) induces remodeling and enhances TH2-mediated sensitization and inflammation in the lung. *Nat Med*. 2004;10(10):1095-1103. doi:10.1038/nm1105

17. Green CE, Turner AM. The role of the endothelium in asthma and chronic obstructive pulmonary disease (COPD). *Respir Res*. 2017;18:20. doi:10.1186/s12931-017-0505-1

18. Dullaers M, Schuijs MJ, Willart M, et al. House dust mite–driven asthma and allergen-specific T cells depend on B cells when the amount of inhaled allergen is limiting. *J Allergy Clin Immunol*. 2017;140(1):76-88.e7. doi:10.1016/j.jaci.2016.09.020

19. Yasuda Y, Nagano T, Kobayashi K, Nishimura Y. Group 2 Innate Lymphoid Cells and the House Dust Mite-Induced Asthma Mouse Model. *Cells*. 2020;9(5):1178. doi:10.3390/cells9051178

20. Banafea GH, Bakhashab S, Alshaibi HF, Natesan Pushparaj P, Rasool M. The role of human mast cells in allergy and asthma. *Bioengineered*. 13(3):7049-7064. doi:10.1080/21655979.2022.2044278

21. Stone KD, Prussin C, Metcalfe DD. IgE, Mast Cells, Basophils, and Eosinophils. *J Allergy Clin Immunol*. 2010;125(2 Suppl 2):S73-S80. doi:10.1016/j.jaci.2009.11.017

22. Méndez-Enríquez E, Hallgren J. Mast Cells and Their Progenitors in Allergic Asthma. *Front Immunol*. 2019;10. doi:10.3389/fimmu.2019.00821

23. Barletta KE, Cagnina RE, Wallace KL, Ramos SI, Mehrad B, Linden J. Leukocyte compartments in the mouse lung: Distinguishing between marginated, interstitial, and alveolar cells in response to injury. *J Immunol Methods*. 2012;375(1):100-110. doi:10.1016/j.jim.2011.09.013

24. Rodero MP, Poupel L, Loyher PL, et al. Immune surveillance of the lung by migrating tissue monocytes. *eLife*. 4:e07847. doi:10.7554/eLife.07847

25. Stahnke S, Döring H, Kusch C, et al. Loss of Hem1 disrupts macrophage function and impacts migration, phagocytosis, and integrin-mediated adhesion. *Curr Biol*. 2021;31(10):2051-2064.e8. doi:10.1016/j.cub.2021.02.043

26. Mesnil C, Raulier S, Paulissen G, et al. Lung-resident eosinophils represent a distinct regulatory eosinophil subset. *J Clin Invest*. 2016;126(9):3279-3295. doi:10.1172/JCI85664

27. Woo LN, Guo WY, Wang X, et al. A 4-Week Model of House Dust Mite (HDM) Induced Allergic Airways Inflammation with Airway Remodeling. *Sci Rep*. 2018;8(1):6925. doi:10.1038/s41598-018-24574-x

28. Plantinga M, Guilliams M, Vanheerswynghels M, et al. Conventional and monocyte-derived CD11b(+) dendritic cells initiate and maintain T helper 2 cell-mediated immunity to house dust mite allergen. *Immunity*. 2013;38(2):322-335. doi:10.1016/j.immuni.2012.10.016

29. Abu Khweek A, Kim E, Joldrichsen MR, Amer AO, Boyaka PN. Insights Into Mucosal Innate Immune Responses in House Dust Mite-Mediated Allergic Asthma. *Front Immunol*. 2020;11. doi:10.3389/fimmu.2020.534501

30. Muehling LM, Lawrence MG, Woodfolk JA. Pathogenic CD4+ T cells in patients with asthma. *J Allergy Clin Immunol*. 2017;140(6):1523-1540. doi:10.1016/j.jaci.2017.02.025

31. Malaviya R, Zhou Z, Raymond H, et al. Repeated exposure of house dust mite induces progressive airway inflammation in mice: Differential roles of CCL17 and IL-13. *Pharmacol Res Perspect*. 2021;9(3):e00770. doi:10.1002/prp2.770

32. Scott G, Asrat S, Allinne J, et al. IL-4 and IL-13, not eosinophils, drive type 2 airway inflammation, remodeling and lung function decline. *Cytokine*. 2023;162:156091. doi:10.1016/j.cyto.2022.156091

33. Finkelman FD, Hogan SP, Khurana Hershey GK, Rothenberg ME, Wills-Karp M. Importance of Cytokines in Murine Allergic Airway Disease and Human Asthma. *J Immunol Baltim Md 1950*. 2010;184(4):1663-1674. doi:10.4049/jimmunol.0902185

34. Pope SM, Brandt EB, Mishra A, et al. IL-13 induces eosinophil recruitment into the lung by an IL-5– and eotaxin-dependent mechanism. *J Allergy Clin Immunol*. 2001;108(4):594-601. doi:10.1067/mai.2001.118600

35. Holgate ST, Bodey KS, Janezic A, Frew AJ, Kaplan AP, Teran LM. Release of RANTES, MIP-1 alpha, and MCP-1 into asthmatic airways following endobronchial allergen challenge. *Am J Respir Crit Care Med*. 1997;156(5):1377-1383. doi:10.1164/ajrccm.156.5.9610064

36. Koya T, Takeda K, Kodama T, et al. RANTES (CCL5) Regulates Airway Responsiveness after Repeated Allergen Challenge. *Am J Respir Cell Mol Biol*. 2006;35(2):147-154. doi:10.1165/rcmb.2005-0394OC

37. Kobayashi Y, Konno Y, Ueki S, Tomoda K, Kanda A. MIP-1β is associated with eosinophilic airway inflammation. *Eur Respir J*. 2016;48(suppl 60). doi:10.1183/13993003.congress-2016.PA934

38. Chesné J, Braza F, Mahay G, Brouard S, Aronica M, Magnan A. IL-17 in severe asthma. Where do we stand? *Am J Respir Crit Care Med*. 2014;190(10):1094-1101. doi:10.1164/rccm.201405-0859PP

39. Song C, Luo L, Lei Z, et al. IL-17-producing alveolar macrophages mediate allergic lung inflammation related to asthma. *J Immunol Baltim Md 1950*. 2008;181(9):6117-6124. doi:10.4049/jimmunol.181.9.6117

40. O'Garra A, Barrat FJ, Castro AG, Vicari A, Hawrylowicz C. Strategies for use of IL-10 or its antagonists in human disease. *Immunol Rev*. 2008;223:114-131. doi:10.1111/j.1600-065X.2008.00635.x

41. Till SJ, Francis JN, Nouri-Aria K, Durham SR. Mechanisms of immunotherapy. *J Allergy Clin Immunol*. 2004;113(6):1025-1034; quiz 1035. doi:10.1016/j.jaci.2004.03.024

42. Hino A, Fukuyama S, Kataoka K, Kweon MN, Fujihashi K, Kiyono H. Nasal IL-12p70 DNA Prevents and Treats Intestinal Allergic Diarrhea1. *J Immunol*. 2005;174(11):7423-7432. doi:10.4049/jimmunol.174.11.7423

43. Cyphert-Daly JM, Yang Z, Ingram JL, Tighe RM, Que LG. Physiologic response to chronic house dust mite exposure in mice is dependent on lot characteristics. *J Allergy Clin Immunol*. 2019;144(5):1428-1432.e8. doi:10.1016/j.jaci.2019.07.019

44. Weiss K, Wanner N, Queisser K, et al. Barrier Housing and Gender Effects on Allergic Airway Disease in a Murine House Dust Mite Model. *ImmunoHorizons*. 2021;5(1):33-47. doi:10.4049/immunohorizons.2000096

45. Kim DI, Song MK, Lee K. Comparison of asthma phenotypes in OVA-induced mice challenged via inhaled and intranasal routes. *BMC Pulm Med*. 2019;19(1):241. doi:10.1186/s12890-019-1001-9

46. Mostafa DHD, Hemshekhar M, Piyadasa H, et al. Characterization of sex-related differences in allergen house dust mite-challenged airway inflammation, in two different strains of mice. *Sci Rep*. 2022;12(1):20837. doi:10.1038/s41598-022-25327-7

47. Jia A, Wang Y, Sun W, et al. Comparison of the roles of house dust mite allergens, ovalbumin and lipopolysaccharides in the sensitization of mice to establish a model of severe neutrophilic asthma. *Exp Ther Med*. 2017;14(3):2126-2134. doi:10.3892/etm.2017.4776

48. Jartti T, Bønnelykke K, Elenius V, Feleszko W. Role of viruses in asthma. *Semin Immunopathol*. 2020;42(1):61-74. doi:10.1007/s00281-020-00781-5

49. Martinez J, Cook DN. What's the deal with efferocytosis and asthma? *Trends Immunol*. 2021;42(10):904-919. doi:10.1016/j.it.2021.08.004

50. Fricker M, Gibson PG. Macrophage dysfunction in the pathogenesis and treatment of asthma. *Eur Respir J*. 2017;50(3). doi:10.1183/13993003.00196-2017